



HAL
open science

Leaf traits and temperature shape the elevational patterns of phyllosphere microbiome

Xing Wang, Zuoqiang Yuan, Arshad Ali, Teng Yang, Fei Lin, Zikun Mao, Ji Ye, Shuai Fang, Zhanqing Hao, Yoann Le Bagousse-Pinguet

► **To cite this version:**

Xing Wang, Zuoqiang Yuan, Arshad Ali, Teng Yang, Fei Lin, et al.. Leaf traits and temperature shape the elevational patterns of phyllosphere microbiome. *Journal of Biogeography*, 2023, 50 (12), pp.2135-2147. 10.1111/jbi.14719 . hal-04271969

HAL Id: hal-04271969

<https://hal.science/hal-04271969>

Submitted on 6 Nov 2023

HAL is a multi-disciplinary open access archive for the deposit and dissemination of scientific research documents, whether they are published or not. The documents may come from teaching and research institutions in France or abroad, or from public or private research centers.

L'archive ouverte pluridisciplinaire **HAL**, est destinée au dépôt et à la diffusion de documents scientifiques de niveau recherche, publiés ou non, émanant des établissements d'enseignement et de recherche français ou étrangers, des laboratoires publics ou privés.

Elevational patterns and drivers of phyllosphere microbial diversity

Journal:	<i>Journal of Biogeography</i>
Manuscript ID	JB1-22-0288.R1
Wiley - Manuscript type:	Research Article
Date Submitted by the Author:	20-Oct-2022
Complete List of Authors:	<p>Wang, Xing; CAS Key Laboratory of Forest Ecology and Management Institute of Applied Ecology Chinese Academy of Sciences Shenyang China</p> <p>Yuan, zuoqiang; CAS Key Laboratory of Forest Ecology and Management Institute of Applied Ecology Chinese Academy of Sciences Shenyang China; Northernwest Polytechnical University, School of Ecology and Environment</p> <p>Ali, Arshad; Forest Ecology Research Group College of Life Sciences Hebei University Baoding 071002 Hebei China</p> <p>Yang, Teng; State Key Laboratory of Soil and Sustainable Agriculture Institute of Soil Science Chinese Academy of Sciences East Beijing Road 71 Nanjing 210008 China</p> <p>Lin, fei; CAS Key Laboratory of Forest Ecology and Management Institute of Applied Ecology Chinese Academy of Sciences Shenyang China</p> <p>Mao, Zikun; CAS Key Laboratory of Forest Ecology and Management Institute of Applied Ecology Chinese Academy of Sciences Shenyang China</p> <p>Ye, Ji; CAS Key Laboratory of Forest Ecology and Management Institute of Applied Ecology Chinese Academy of Sciences Shenyang China</p> <p>Fang, Shuai; CAS Key Laboratory of Forest Ecology and Management Institute of Applied Ecology Chinese Academy of Sciences Shenyang China</p> <p>Hao, Zhanqing; School of Ecology and Environment Northernwest Polytechnical University China</p> <p>Wang, xugao; CAS Key Laboratory of Forest Ecology and Management Institute of Applied Ecology Chinese Academy of Sciences Shenyang China; Institute of Applied Ecology Chinese Academy of Sciences, Key Laboratory of Terrestrial Ecosystem Carbon Neutrality</p> <p>Pinguet, Yoann; Aix Marseille Univ CNRS Avignon Université IRD IMBE Technopôle Arbois-Méditerranée Bât Villemin –BP80 Aix-en-Provence cedex 04 France</p>
Key Words:	Biodiversity, Climate, Elevation, Plant functional traits, Plant-microbe associations, Microbial ecology

1
2
3
4
5
6
7
8
9
10
11
12
13
14
15
16
17
18
19
20
21
22
23
24
25
26
27
28
29
30
31
32
33
34
35
36
37
38
39
40
41
42
43
44
45
46
47
48
49
50
51
52
53
54
55
56
57
58
59
60



Elevational patterns and drivers of phyllosphere microbial diversity

Xing Wang^{1,2}, Zuoqiang Yuan^{1,3*}, Arshad Ali⁴, Teng Yang⁵, Fei Lin¹, Zikun Mao¹, Ji Ye¹, Shuai Fang¹, Zhanqing Hao³, Xugao Wang¹, Yoann Le Bagousse-Pinguet⁶

¹CAS Key Laboratory of Forest Ecology and Management, Institute of Applied Ecology, Chinese Academy of Sciences, Shenyang, China

²University of Chinese Academy of Sciences, Beijing 100049, China

³School of Ecology and Environment, Northernwest Polytechnical University, China

⁴Forest Ecology Research Group, College of Life Sciences, Hebei University, Baoding 071002, Hebei, China

⁵State Key Laboratory of Soil and Sustainable Agriculture, Institute of Soil Science, Chinese Academy of Sciences, East Beijing Road 71, Nanjing 210008, China

⁶Aix Marseille Univ, CNRS, Avignon Université, IRD, IMBE, Technopôle Arbois-Méditerranée Bât. Villemin –BP80, Aix-en-Provence cedex 04, France

Author for correspondence: Zuoqiang Yuan (zqyuan@iae.ac.cn)

1
2
3 **17 Abstract:**
4

5 **18 Aim:** Phyllosphere microbial diversity (PMD) is a central biodiversity component for plant health,
6
7
8 **19** distribution, and ecosystem functioning. Yet, how climate and leaf functional traits of host plants
9
10
11 **20** simultaneously shape elevational patterns of PMD is unclear; but it could improve our ability to
12
13 **21** predict plant performance and distributions and ecosystem functioning under environmental
14
15 **22** changes.
16

17 **23 Location:** Temperate forests of Changbai Mountain Natural Reserve, China
18

19 **24 Methods:** We investigated changes in the species richness and Shannon's diversity of endo- and
20
21
22
23
24
25
26
27
28
29
30
31
32
33
34
35
36
37
38
39
40
41
42
43
44
45
46
47
48
49
50
51
52
53
54
55
56
57
58
59
60

28 Results: We observed a monotonous decline in PMD with increasing elevation, contrasting with
29
30
31
32
33
34
35
36
37
38
39
40
41
42
43
44
45
46
47
48
49
50
51
52
53
54
55
56
57
58
59
60

37 Main conclusions: Our results suggest considering both direct and mediating effects of plant traits
38
39
40
41
42
43
44
45
46
47
48
49
50
51
52
53
54
55
56
57
58
59
60

1
2
3 40 study also offers a trait-based attempt to disentangle the effects of biotic and abiotic filters in
4
5 41 shaping endo- and epiphytic phyllosphere microbial diversity along an elevational gradient.
6

7
8 42 **Keywords:** Biodiversity, Climate, Elevation, Plant functional traits, Plant-microbe associations,
9
10 43 Microbial ecology.
11
12
13
14
15
16
17
18
19
20
21
22
23
24
25
26
27
28
29
30
31
32
33
34
35
36
37
38
39
40
41
42
43
44
45
46
47
48
49
50
51
52
53
54
55
56
57
58
59
60

For Peer Review

45 Introduction

46 The phyllosphere – the aboveground part of plants – constitutes the largest surface area that
47 microbes inhabit on Earth, and is being estimated to be twice of the global land area (Vorholt,
48 2012; Zhu et al., 2021). The phyllosphere homes a large variety of phyllosphere microbes,
49 including endophytic and epiphytic fungi and bacteria (Phyllosphere Microbial Diversity;
50 hereafter PMD) (Vorholt, 2012). PMD is a central biodiversity component, largely involved in
51 plant health and performance, influencing ecosystem functioning and supporting crop production
52 (Vacher et al., 2016; Wang et al., 2021). Occurring at the interface between the leaf and the
53 atmosphere, PMD perceives the influences of abiotic (climate) and local biotic conditions (i.e. the
54 host plants). Investigating how PMD simultaneously responds to abiotic and biotic conditions
55 constitutes a great opportunity to better understand how the multiple environmental drivers shape
56 phyllosphere microbial communities, and may offer opportunities to better predict plant
57 performance and distribution, as well as ecosystem functioning under [global](#) environmental
58 changes.

59 Mountain ranges [harbor](#) many species endemic to high-elevation habitats, and exhibit multiple
60 but steep environmental changes at relatively small horizontal distances (Bryant et al., 2008;
61 Körner, 2000). For these reasons, elevational diversity gradients received considerable attention
62 (Rahbek et al., 2019). Organismal diversity could follow the early reported decreasing pattern with
63 higher elevation (Von Humboldt & Bonpland, 1805), following the notion that the environment
64 selects for a narrow and similar set of species (The environmental filtering hypothesis) (Le
65 Bagousse-Pinguet et al., 2017; Weiher, Clarke, & Keddy, 1998). However, a hump-shaped pattern
66 of diversity peaking at mid-elevations is likely to occur most commonly (Rahbek, 1995). These
67 diversity patterns have been documented for multiple taxa, such as soil microbes (Bryant et al.,

1
2
3 68 2008), insects (Machac, Janda, Dunn, & Sanders, 2011; Sanders, 2002), birds (Duclos, DeLuca,
4
5 69 & King, 2019), and plants (Grytnes & Beaman, 2006; Le Bagousse-Pinguet et al., 2018). However,
6
7
8 70 we yet lack a clear understanding on how elevational - and underlying abiotic - gradients shape
9
10 71 endo- and epiphytic PMD simultaneously. Determining whether PMD follow any particular
11
12 72 pattern, and whether they follow the trends observed for other taxa may not only help to better
13
14
15 73 understand the drivers shaping PMD patterns, but also extend, confirm, or refine the existing
16
17 74 elevational diversity gradients to unknown taxa.

18
19 75 Elevational diversity patterns have, yet, barely considered fine-scale biotic filters. For
20
21 76 instance, the presence of cushion plants, either being competitive or offering micro-refuges, could
22
23
24 77 mediate phylogenetic patterns of plant diversity along elevational gradients (Butterfield et al.,
25
26 78 2013; Cavieres et al., 2014; Le Bagousse-Pinguet et al., 2018). Similarly, we could expect that
27
28 79 host species act as an important biotic filter shaping, confounding or even altering the overall
29
30
31 80 elevational patterns of PMD. The selection effect of plant host on phyllosphere microbes largely
32
33 81 depends on plant attributes (i.e. plant functional traits) (Carvalho & Castillo, 2018; Jia, Yao, Guo,
34
35 82 Wang, & Chai, 2020; Leveau, 2019; Vacher et al., 2016). Because plant functional traits relate to
36
37 83 how species acquire and conserve resources (Díaz et al., 2007), they represent good proxies of the
38
39
40 84 local biotic environment where phyllosphere microbial communities survive. In such a context,
41
42 85 phyllosphere bacterial communities were tightly coupled with leaf dry matter content and leaf area,
43
44 86 two plant functional traits involved in resource uptake (Kembel et al., 2014), while fungal
45
46 87 communities mostly responded to leaf nitrogen content and specific leaf area (Kembel & Mueller,
47
48 88 2014). However, host plants and their traits may exert greater impacts on the microbe colonization
49
50
51 89 of internal tissues than on that of leaf surfaces, leading to potential distinct responses of epiphytic
52
53
54 90 and endophytic microbes to the environment (Yao, Sun, He, Li, & Guo, 2020; Yao et al., 2019).

1
2
3 91 For instance, endophytic fungi directly acquire nutrients from inner plant tissues, whereas
4
5 92 epiphytic microbes in contact with the external environment mostly depend on the amount of
6
7
8 93 nutrients either exuded from leaves or depositing from the atmosphere (Inácio et al., 2002). Hence,
9
10 94 deciphering the relative effects of abiotic and biotic filters simultaneously shaping endo- and
11
12 95 epiphytic PMD patterns remains unclear (Agler et al., 2016; Cordier et al., 2012; Wei et al., 2022),
13
14
15 96 and constitutes an important step in our understanding of plant – microbe associations.

16
17 97 Associations (covariations) between bacteria and fungi can arise from a diverse range of
18
19 98 interactions, from negative to neutral or even positive. Negative associations could occur as a
20
21 99 signature of competition for space and resources (Bahram et al. 2018), while niche partitioning
22
23 100 may promote positive covariations as a result of fitness differences among organisms (Bruno,
24
25 101 Stachowicz, & Bertness, 2003). For instance, fungal organic matter degradation has been shown
26
27 102 to benefit bacteria (Boer, Folman, Summerbell, & Boddy, 2005). Yet, whether and how abiotic
28
29 103 and biotic filters shape PMD associations remains poorly investigated (Agler et al., 2016; Cordier
30
31 104 et al., 2012; Wei et al., 2022), even though describing how complex interactions among microbial
32
33 105 communities could largely matter for the health of plants.

34
35
36
37 106 Here, we investigated changes in the species richness and Shannon's diversity index of endo-
38
39 107 and epi-phytic phyllosphere fungi and bacteria, and their covariations, along a steep 1150 m
40
41 108 elevational gradient. We addressed the following questions and associated hypotheses: Q1) Does
42
43 109 PMD exhibit particular elevational patterns? H1) We hypothesized that the diversity of
44
45 110 phyllosphere microbes follows a mid-elevational gradient pattern, corresponding to the most
46
47 111 common pattern observed across taxa. Q2) Do phyllosphere endo- and epiphytic microbes respond
48
49 112 similarly to abiotic and biotic filters? H2) We hypothesized that endophytic microbes are more
50
51 113 sensitive to the biotic filter (i.e., host plant traits), whereas epiphytic microbes mostly respond to
52
53
54
55
56
57
58
59
60

1
2
3 114 climate. Q3) How do abiotic and biotic filters shape PMD covariations? H3) We hypothesized
4
5 115 prominent negative relationships as a signature of competition for space and resources, and the
6
7
8 116 elevational gradient to modulate these associations.
9

10 117

11 118 **Material and Methods**

12 119 **Study site and climate data**

13
14
15
16
17 120 The study site is located in the Changbai Mountain Natural Reserve (127° 42' to 128° 17' E,
18
19 121 41° 43' to 42° 26' N) in the Jilin province of northeastern China (Fig. 1a), which is one of the
20
21
22 122 largest protected temperate forests around the world (Stone, 2006; Wang et al., 2013). The reserve
23
24 123 covers approximately 200, 000 ha, with an elevation range between 740 and 2691 m a.s.l. The area
25
26 124 is strongly influenced by the monsoon and experiences a temperate continental mountain climate
27
28
29 125 with long, cold winters and warm summers. The predominant soil type of the studied area is Alfisol
30
31 126 according to the US soil taxonomy (Mao et al., 2019; Yang, 1985; Yuan et al., 2013).

32
33 127 The elevational gradient considered in this study ranges from the mountain foot (500 m a.s.l.)
34
35
36 128 to the summit (the volcanic crater lake) (2744 m a.s.l.) (Fig. 1b), where the mean annual
37
38 129 temperature declines from 3.5 to -7.4 °C, but the mean annual precipitation (MAP) increases from
39
40 130 632 to 1154 mm. The elevational gradient encompasses four distinct vegetation zones: the broad-
41
42
43 131 leaved Korean pine (*Pinus koraiensis*) mixed forest (500 m–1100 m), the spruce-fir (*Picea*
44
45 132 *jezoensis* and *Abies nephrolepis*) forest (1100–1800 m), the subalpine birch (*Betula ermanii*) forest
46
47 133 (1800–2000 m) and an alpine tundra zone (above 2100 m). Along with a horizontal distance of
48
49
50 134 about 40 km, these four forest types represent a condensed picture of the array of vegetation
51
52 135 landscapes from the temperate zone to the polar region (Shao, Schall, & Weishampel, 1994; Yang,
53
54 136 1985). [Data of mean annual temperature and precipitation were retrieved from \(Shen et al., 2014;](#)
55
56
57
58
59
60

1
2
3 137 [Shen et al., 2013](#))

4
5 138

6
7
8 139 **Leaf sampling**

9
10 140 Leaf samples were collected in August 2020 at 800, 1000, 1200, 1400 1600, 1800 and 1950 m, i.e.

11
12 141 at all representative forest zones along the studied elevational gradient (Table S1). [At each](#)

13
14 142 [elevation, we established five 50×50m plots that had an interval of 50 m and sampled 5 samples](#)

15
16 143 [of each tree species from each elevation \(one sample per plot\) \(Fig1 c\). Because the number of](#)

17
18 144 [dominant tree species differed among elevations \(there are 30, 20, 5,10, 20, 10 and 5 samples from](#)

19
20 145 [the low to high elevation\), the total number of samples was not same among elevations \(Fig. 1b\).](#)

21
22 146 In each plot, leaves without signs of disease or feeding damage were collected on one adult tree of

23
24 147 each of the dominant species (Table S2). The specialized worker climbed upward the canopy of

25
26 148 each tree by foot hook and took three branches from four directions using sterilized scissors. About

27
28 149 80 gram of healthy leaves were taken using sterile gloves and then subdivided into two samples.

29
30 150 One sample was stored at 4 °C to determine the leaf morphological and chemical properties,

31
32 151 while the other sample was stored at –80 °C before DNA extraction. A total of 100 leaf samples

33
34 152 were sampled from ten tree species (n=100, some species are distributed at multiple elevations).

35
36 153

37
38
39 154 **Leaf functional traits**

40
41 155 We measured 13 common leaf morphological and chemical traits related to life history and nutrient

42
43 156 and water-use efficiencies (Table S3 & Fig. S1), following standard protocols (Pérez-

44
45 157 Harguindeguy et al., 2013). Leaf morphological traits, such as specific leaf area (SLA), reflect

46
47 158 light interception ability and trade-offs between the longevity of the plant tissues and construction

48
49 159 cost, whereas leaf chemical traits such as leaf carbon (LCC) and leaf nitrogen content (LNC) reflect

50
51
52
53
54
55
56
57
58
59
60

1
2
3 160 photosynthetic and growth ability (Chave et al., 2009). Leaf area (LA) was calculated using a
4
5 161 portable scanner (Canon LiDE 110, Tokyo, Japan) and Image-Pro Plus 6.0 software (Media
6
7 162 Cybernetics, USA). The mass of dried leaf samples (LDMC) with an accuracy of 0.1 mg was
8
9 163 estimated after oven-drying at 65 °C for 48 hours at a constant mass. SLA was calculated as the
10
11 164 ratio of projected leaf area to leaf dry mass. A RETSCH MM400 (RETSCH, GmbH, Haan,
12
13 165 Germany) was then used to ground the oven-dried leaf samples into a fine powder. Leaf carbon
14
15 166 and nitrogen contents were measured using an elemental analyzer (Vario EL III, Elementar, Hanau,
16
17 167 Germany. Leaf stable carbon (LCC_{13}) and nitrogen isotope composition (LNC_{15}) was analyzed
18
19 168 using the isotopic Cavity-Ring Down Spectrometer with the Combustion Module (CMCRDS
20
21 169 system, Picarro, CA, USA). We also measured the following chemical elements: leaf phosphorus
22
23 170 content (LPC), leaf potassium content (LKC), leaf copper content (LCuC), leaf calcium content
24
25 171 (LCaC) and leaf zinc content (LZnC) using an ICP Optima 8000 (Perkin-Elmer, Waltham, MA,
26
27 172 USA).

28
29 173 We used the nail-polish imprint method (Zhao, Chen, Brodribb, & Cao, 2016) to estimate leaf
30
31 174 stomatal character. Six leaves were randomly selected from each sample, and the nail polish was
32
33 175 applied to the center of the abaxial leaf surface. After the nail polish is dried, the polish was then
34
35 176 stripped using sellotape and mounted onto a glass slide. Microphotographs were photographed
36
37 177 using a Classica SK200 Digital light microscope (Motic China Group Co., Ltd, China). 3-5 visual
38
39 178 fields were randomly selected for each sample in a 40-fold objective lens and a 10-fold eye lens.
40
41 179 Leaf stomatal area (LSA) was calculated as the mean value of the product of the length of the long
42
43 180 axis and the length of the short axis of the five stomata selected in the random field using Image-
44
45 181 Pro Plus 6.0 software (Media Cybernetics, USA).

46
47
48
49
50
51
52
53
54 182

183 **Leaf DNA extraction and sequencing**

184 Phyllosphere epiphytic microbes were washed from leaf surfaces according to the standard
185 protocols (Yao et al., 2020; Yao et al., 2019). Five g of leaf samples were placed in sterile tubes
186 and 10 ml of sterile cooled TE buffer (10 mM Tris-HCl, 1 mM EDTA, pH 7.5) was added to each
187 gram of samples. Samples were then washed by ultrasonic for 1 min and whirled for 10 s, and
188 repeated twice. The liquids obtained after two cleanings were mixed and passed through a 0.2 µm
189 sterile filter membrane (SUPOR, Pall Corporation). The filtered membrane was transferred to the
190 freezer at -80 °C for analysis (Herrmann, Geesink, Richter, & Küsel, 2021). Samples of endophyte
191 microbes were isolated from the same plant leaves used for isolating epiphytes. The leaves were
192 submerged for 1 min with 75% ethanol, 3.25% sodium hypochlorite for 3 min, 75% ethanol for 30
193 s, and eventually rinsed 3 times with sterile distilled water. [Each sample was ground in liquid
194 nitrogen using a mortar and pestle, and then only 5 g of leaf powder was retained for DNA
195 extraction](#) (Bodenhausen, Horton, & Bergelson, 2013).

196 Total genomic DNA was extracted by the FastDNA® SPIN Kit (Qbiogene, Irvine, CA)
197 according to the manufacturer's instructions. The DNA extract was checked on 1% agarose gel,
198 and DNA concentration and purity were determined with NanoDrop 2000 UV-vis
199 spectrophotometer (Thermo Scientific, Wilmington, USA). For bacteria, we targeted V5-V7
200 region of the 16S rRNA gene, using 799F (AACMGGATTAGATACCCKG) and 1193R
201 (ACGTCATCCCCACCTTCC). [Two step PCR were used to amplify phyllosphere endophytic
202 bacteria. This method and the primer we choose can guarantee good coverage of endophytic
203 bacteria taxa](#) (Bulgarelli et al., 2015; Bulgarelli et al., 2012; Giangacomo, Mohseni, Kovar, &
204 [Wallace, 2021; Lundberg et al., 2012](#)). The PCR amplification was performed as follows: initial
205 denaturation step at 95°C for 3 min, the targeted region was amplified by 27 cycles of 95°C for 30

1
2
3 206 s, 55°C for 30 s and 72°C for 45 s, followed by a final elongation step of 10 min at 72°C with the
4
5 207 799F and 1392R (ACGGGCGGTGTGTRC) primers. With sterile deionized water, the initial PCR
6
7 208 product was diluted by a factor of 50. 1.0 μ L of the diluted solution was used. The second-step
8
9 209 primers were 799F-1193R and identical conditions to the first step except for the number of PCR
10
11 210 cycles that was lowered to 13. For fungi, we targeted the ITS1 region of the rRNA operon, using
12
13 211 the ITS1F (CTTGGTCATTTAGAGGAAGTAA) and ITS2R (GCTGCGTTCTTCATCGATGC).
14
15 212 The PCR amplification was performed as follows: initial denaturation at 95 °C for 3 min,
16
17 213 followed by 35 cycles of denaturing at 95 °C for 30 s, annealing at 55 °C for 30 s and extension
18
19 214 at 72 °C for 45 s, and single extension at 72 °C for 10 min, and end at 10 °C. PCR amplification
20
21 215 was performed for both the 16 S rRNA gene and the ITS1 region with 20 μ l reaction system,
22
23 216 containing 5 \times TransStart FastPfu buffer 4 μ L, 2.5 mM dNTPs 2 μ L, forward primer (5 μ M) 0.8
24
25 217 μ L, reverse primer (5 μ M) 0.8 μ L, TransStart FastPfu DNA Polymerase 0.4 μ L, template DNA 10
26
27 218 ng, and finally ddH₂O up to 20 μ L. PCR reactions were performed in triplicate. The PCR product
28
29 219 was extracted from 2% agarose gel and purified using the AxyPrep DNA Gel Extraction Kit
30
31 220 (Axygen Biosciences, Union City, CA, USA) according to the manufacturer's instructions and
32
33 221 quantified using Quantus™ Fluorometer (Promega, USA). The raw data were sequenced on an
34
35 222 Illumina NovaSeq PE250 platform (Illumina, San Diego, USA) by Majorbio Bio-Pharm
36
37 223 Technology Co. Ltd. (Shanghai, China).
38
39
40
41
42
43
44
45
46
47

225 **Bioinformatic analyses**

48
49 226 The raw gene sequencing reads were filtered using QIIME (version 1.7)
50
51 227 (<http://qiime.org/tutorials/tutorial.html>). Low-quality sequences (length<200 bp), ambiguous bases>0,
52
53 228 average base quality score<25) were removed. Samples were distinguished according to the
54
55
56
57
58
59
60

barcode and primers, and the sequence direction was adjusted. The amplicon length ranges for 16S are 593bp (the first PCR) and 394bp (the second PCR), and the amplicon length ranges for ITS is 300bp (Yang et al., 2019). Only overlapping sequences longer than 10 bp were assembled according to their overlapped sequence. The maximum mismatch ratio of the overlap region is 0.2. Reads that could not be assembled were discarded; Samples were distinguished according to the barcode and primers, and the sequence direction was adjusted, exact barcode matching, 2 nucleotide mismatch in primer matching. The sequences were then clustered into operational taxonomic units (OTUs) with 97% similarity cutoff using UPARSE version 7.1 (Edgar, 2013), and chimeric sequences were identified and removed. The taxonomy of each OTU representative sequence of bacteria and fungi was assigned by RDP Classifier version 2.2 (Wang, Garrity, Tiedje, & Cole, 2007) against the Silva v138 with a confidence cut-off (P) value of 0.80 and UNITE 8.0 with a confidence cut-off (P) value of 0.70, respectively. The OTUs that were not classified into bacteria or fungi were removed. In total, we obtained 12,218,626 and 11,031,668 high-quality sequences for fungi and bacteria separately. After rarefying all samples to an equal sequencing depth (21898 reads per sample), the fungal and bacterial communities included 3110 and 5231 OTUs, respectively. The proportion of Chloroplasts (4/3173) and Mitochondria (30/3173) in the total number of OTUs was acceptable, and did not affect our analysis.

Statistical analyses

To evaluate the elevational patterns of PMD, we conducted linear mixed models with the Shannon index (H) (average value of each plot) and negative binomial generalized linear models with the richness (S) (average value of each plot) of all (i.e., epiphytic + endophytic), endo- and epiphytic bacteria and fungi as response variables, whereas elevation and elevation² (i.e. to test for potential

1
2
3 252 humped-shaped relationships) as predictors, and the [plot as a random factor](#). We used negative
4
5 253 binomial generalized linear models to account for the richness of microbes (e.g. the number of
6
7 254 OTUs) in count data (Shrestha, Su, Xu, & Wang, 2018). Models were sorted and compared
8
9 255 according to the Akaike Information Criterion (AIC) and the likelihood ratio test.
10
11

12 256 [We performed a heatmap plot to illustrate the relationships between plant functional traits and](#)
13
14 257 [specific microbial taxa by “corrplot” package \(Wei et al., 2017\)](#). We further performed a principal
15
16 258 component analysis (PCA) on the nine least correlated leaf traits (over the 13 traits originally
17
18 259 considered; Fig. S1). This approach approximates the functional space that species occupy and
19
20 260 defines their position in multi-dimensional trait space (Devictor et al., 2010). The first axis of PCA
21
22 261 (FT_{PC1}) explained 46.9% of the total variation in trait variables. This axis mainly correlated with
23
24 262 high leaf area and SLA (Table S4), thus discriminating leaf traits associated with the leaf economic
25
26 263 spectrum (LES; Wright *et al.*, 2004). The second axis (FT_{PC2}) explained 28.7% of the total
27
28 264 variation in trait variables, and mainly correlated with micronutrients such as leaf copper and zinc
29
30 265 contents. The two PCA axes were used in subsequent analyses because they are independent
31
32 266 variables at the species level and reflect important leading dimensions of the species niche (Gross
33
34 267 *et al.*, 2013).
35
36
37
38
39

40 268 To evaluate the simultaneous effects of abiotic (climate) and biotic (leaf traits) conditions on
41
42 269 endo- and epiphytic PMD, we performed linear mixed models with H and with S of all, endo- and
43
44 270 epiphytic bacteria and fungi as response variables. We included MAT and MAT^2 as climate
45
46 271 predictors (MAP was considered, but removed due to its high correlation with MAT and less
47
48 272 importance in the models; Fig. S1), FT_{PC1} and FT_{PC2} as biotic predictors, and site included as a
49
50 273 random factor. Response variables were log-transformed when necessary to normalize data
51
52 274 distribution prior to analyses to meet the assumptions of the test used. All predictors were
53
54
55
56
57
58
59
60

1
2
3 275 standardized using the Z-score to interpret parameter estimates on a comparable scale. Models
4
5 276 were ranked according to the lowest AICc, and retained within $\Delta AIC < 2$. Standardized regression
6
7
8 277 coefficients (β) were obtained using a model averaging approach. Since all predictors and response
9
10 278 variables were standardized, an analogue of the variance decomposition analysis was applied to
11
12 279 obtain the relative importance of each predictor based on the marginal R^2 , which can be simply
13
14
15 280 calculated as the ratio between its standardized regression coefficient and the sum of all
16
17 281 coefficients, and expressed in % (Le Bagousse-Pinguet et al., 2019; Yuan et al., 2021).

18
19 282 Finally, piecewise structural equation models (pSEMs) were performed to investigate direct
20
21 283 and indirect pathways of the abiotic and biotic influences on PMD and their associations (the
22
23 284 conceptual model is provided in Fig. S4). Each predictor's indirect impact was estimated by
24
25
26 285 combining the standardized direct effect of a predictor on a mediator with the direct influence of
27
28 286 a mediator on the response variable. The total effect of predictors is calculated as the sum of direct
29
30
31 287 and indirect effects (Yuan et al., 2020). Based on a priori theoretical knowledge, we hypothesized
32
33 288 that functional traits and climate factors simultaneously would have a direct impact on PMD (e.g.
34
35 289 S of bacteria and fungi), and climate factors also would have an indirect impact on PMD via
36
37
38 290 altering functional traits. We also considered potential relationships between bacteria and fungi to
39
40 291 evaluate the strength and direction of their associations using **linear mixed models** in pSEM
41
42 292 analyses. Site was used as a random factor. Model parameters and fit were assessed using Fisher's
43
44
45 293 C statistic. Models with adequate fit to the data had a Fisher's C statistic with $p > 0.05$ (Shipley,
46
47 294 2009). The pSEM analyses were performed using “piecewiseSEM” package (Lefcheck, 2016).
48
49 295 The pSEMs were tested for S and H of phyllosphere epiphytic, endophytic and all microbial groups
50
51 296 (epiphytic + endophytic).

52
53
54 297 All statistical analyses were performed in the R 4.1.0 software (<http://www.r-project.org/>).

298 The negative binomial generalized linear models were conducted using the *MASS* package. The
299 linear mixed models were conducted using the *lme4* package, and model selection was performed
300 using the “dredge” function in the *MuMIn* package (Bartoń, 2020).

301

302 Results

303 We found that endo- and epiphytic bacteria were mainly composed of Proteobacteria and
304 Actinomycetes, while phyllosphere fungi were mainly represented by Ascomycetes and
305 Basidiomycetes (Appendix Fig. S2 & S3). Proteobacteria (the most dominant bacterial group)
306 were evenly distributed among the studied tree species, while the dominant groups of fungi
307 (Ascomycetes) were mainly associated to *Larix_gmelinii* and *Betula_ermanii*. The phyllosphere
308 microbes mostly occurred at low (800m) and mid-elevation (1600m).

309 For all studied response variables, the best—fitted models included elevation only as a
310 predictor (Fig.2; Appendix Tables S5 & S6). We observed a linear decrease pattern in richness (S)
311 and Shannon index (H) for both bacterial and fungal communities along the studied elevational
312 gradient. We observed a steeper decline in epiphytic bacterial diversity ($Bacteria_{Epip}$) than in
313 endophytic bacteria ($Bacteria_{Endo}$) (ANOVA test' $P < 0.001$, Fig.1), whereas endophytic fungi
314 ($Fungi_{Endo}$) decreased more dramatically along the elevational gradient than epiphytic fungi
315 ($Fungi_{Endo}$) (ANOVA test' $P < 0.001$).

316 The climate (MAT) and the multiple leaf traits accounted for a fair amount of explained
317 variance across the richness (S) of phyllosphere microbes (from 50 to 66%), and notably for
318 epiphytic fungi (Fig.3f). Mean annual temperature (MAT) explained on average 27% of variations
319 (19%–37%) in S of phyllosphere microbes. The climate (MAT) and the multiple leaf traits
320 explained a slightly higher amount of variance (from 56% to 69%) for the Shannon index (H), and

1
2
3 321 notably for the epiphytic fungi (Fig.S5f). Mean annual temperature (MAT) explained up to 30%
4
5 322 (22%–38%) of variations in H of phyllosphere microbes. MAT was significantly associated with
6
7 323 higher S and H of microbial communities, indicating that higher temperature linearly increased
8
9 324 both the richness and Shannon's diversity of microbes (MAT²: $p > 0.05$). The first axis of PCA on
10
11 325 functional traits (FT_{PC1}) – related to the LES - explained up to 26% (13%–37%) and 28% (15%–
12
13 326 41%) for S and H, respectively. Higher leaf area and SLA (and lower LDMC) thus increased the
14
15 327 S and H of both bacterial and fungal communities. In contrast, the second axis of PCA on
16
17 328 functional traits (FT_{PC2}) accounted for only 1.2% (1.1%–1.4%) of variations in PMD (Fig.3
18
19 329 &Fig.5).

20
21
22
23
24 330 The final pSEMs indicated that all PMD metrics were not only associated with direct
25
26 331 changes in MAT and leaf traits but also through indirect pathways (Fig. 4; Appendix Table S7 &
27
28 332 S8). Indirect effects represented up to 12% of variations in PMD. Phyllosphere bacterial S and H
29
30 333 were thus directly influenced by MAT ($\beta=0.305-0.535$) and FT_{PC1} ($\beta=0.258-0.419$), and indirectly
31
32 334 affected by trait-mediated effects of MAT ($\beta= 0.058-0.094$). The average total impact (all,
33
34 335 endophytic and epiphytic) of MAT on phyllosphere bacterial S and H was 0.485 and 0.504,
35
36 336 respectively. Phyllosphere fungal S and H were directly influenced by MAT ($\beta=0.498-0.603$) and
37
38 337 FT_{PC1} ($\beta=0.333-0.508$), but indirectly affected by trait-mediated effects of MAT ($\beta= 0.074-0.114$).
39
40 338 The average total impact (all, endophytic and epiphytic) of MAT on phyllosphere fungal S and H
41
42 339 index were 0.515 and 0.544, respectively. Also, the effects of MAT and FT_{PC1} on phyllosphere
43
44 340 fungi (0.388-0.603 and 0.333-0.508) were greater than those on phyllosphere bacteria (0.305-0.535
45
46 341 and 0.258-0.424). In sum, the effects of MAT on phyllosphere epiphytic microbes (0.524-0.603)
47
48 342 were greater than those on phyllosphere endophytic microbes (0.305-0.571). The effects of FT_{PC1}
49
50 343 on phyllosphere endophytic microbes (0.417-0.508) were greater than those on phyllosphere
51
52
53
54
55
56
57
58
59
60

1
2
3 344 epiphytic microbes (0.258-0.359). Finally, we did not observe any correlations between bacteria
4
5 345 and fungi, neither for endophytic nor epiphytic microbes ($P>0.05$). In addition, there was no strong
6
7 346 change in the pSEMs results across S and H of phyllosphere epiphytic, endophytic and all
8
9 347 microbial groups (Figs. 4, S6, S7 and S8).
10
11
12 348

14 349 **Discussion**

16
17 350 Here, we investigated the elevational patterns of endo- and epiphytic phyllosphere fungal and
18
19 351 bacterial communities, and whether underlying climate (MAT) and biotic drivers (the leaf traits of
20
21 352 host plants) could explain the observed patterns. We observed a linear decrease in the richness and
22
23 353 Shannon's diversity of fungal and bacterial communities along the studied elevational gradient,
24
25 354 but contrary to expectation, no covariations between microbial communities were observed. The
26
27 355 climate features and leaf plant functional traits shaped the observed monotonous decline of
28
29 356 microbial biodiversity, with a higher sensitivity of endophytic microbes to the biotic filter (host
30
31 357 plant traits) and epiphytic microbes to climate.
32
33
34

35 358 We observed a monotonous decline of phyllosphere microbial diversity with increasing
36
37 359 elevation, contrasting with the hump-shaped biodiversity pattern commonly reported across taxa
38
39 360 (Rahbek, 1995), and notably for soil microbes (Geml et al., 2022; Kotilinek et al., 2017; Rehakova,
40
41 361 Chlumska, & Dolezal, 2011). While restricting our study to areas above 700 m.a.s.l. (i.e. the areas
42
43 362 that are the least impacted by human disturbance) may have limited our ability to detect humped-
44
45 363 shaped patterns, our observed PMD patterns concurred with that of tropical plant species richness
46
47 364 decreasing with elevation (Von Humboldt & Bonpland, 1805); and hence, with the view that the
48
49 365 environmental filtering hypothesis (Le Bagousse-Pinguet et al., 2017; Weiher et al., 1998). Our
50
51 366 result also matched with the clustering patterns observed for phylogenetic diversity with elevation
52
53
54
55
56
57
58
59
60

1
2
3 367 for soil microbes (Bryant et al., 2008), insects (Machac et al., 2011; Smith, Hallwachs, & Janzen,
4
5 368 2014), birds (Graham, Parra, Rahbek, & McGuire, 2009), and somehow for plants (Bryant et al.,
6
7 369 2008; Zhang, Xiao, & Li, 2015). However, we also observed that the monotonous decline of PMD
8
9 370 patterns along the elevational gradient was significantly steeper for epiphytic than endophytic
10
11 371 bacteria; but the inverse was observed for fungal communities. These results highlight the complex
12
13 372 responses of phyllosphere biological groups to environmental gradients, and the importance to
14
15 373 discriminate endo- vs. epiphytic microbial communities if we aim at better understanding and
16
17 374 predicting microbial changes in response to ongoing environmental changes. Altogether, our study
18
19 375 extends our understanding of how elevation shapes the diversity of phyllosphere bacteria and fungi,
20
21 376 and brings new evidence that hump-shaped biodiversity patterns may not be as prevalent as
22
23 377 previously thought along elevational gradients (Guo et al., 2013; Wang et al., 2017).

24
25
26
27
28 378 Our results reveal that temperature (and the highly collinear effect of the mean annual
29
30 379 precipitation (MAP; Appendix Fig. S1)) was a key driver of PMD along the studied gradient, but
31
32 380 it predominantly shaped the elevational patterns of epiphytic organisms. While MAT has been
33
34 381 recognized as one of the main abiotic drivers of soil microbes along elevational gradients
35
36 382 (Nottingham et al., 2018), here we showed that the climate impacts depend on how microbes are
37
38 383 exposed to external conditions (Gomes, Pereira, Benhadi-Marín, Lino-Neto, & Baptista, 2018;
39
40 384 Vacher, Cordier, & Vallance, 2016). The observed positive temperature-diversity relationship
41
42 385 could be explained by the metabolic theory of ecology, i.e., temperature could accelerate the
43
44 386 metabolic rates and biochemical processes of organisms (Brown, Gillooly, Allen, Savage, & West,
45
46 387 2004; Gillooly, Brown, West, Savage, & Charnov, 2001). In addition, we observed that MAT has
47
48 388 a slightly higher impact on the phyllosphere fungal than on bacterial diversity, concurring with the
49
50 389 view that fungi are more sensitive to temperature changes than bacteria (Vacher et al., 2016).
51
52
53
54
55
56
57
58
59
60

1
2
3 390 Altogether, our study warns for the potential changes that phyllosphere microbes could experience,
4
5 391 and the potential for this central biodiversity component to further alter plant health, diversity and
6
7 392 ecosystem functioning under global environmental changes such as warming.
8
9

10 393 We found a significant effect of leaf functional traits on elevational patterns of PMD. Our
11
12 394 result points toward the importance of the functional attributes of host plants for PMD, while we
13
14 395 even did not consider plant phylogeny, a biotic driver that encompasses unmeasured biological
15
16 396 traits (Flynn, Mirotchnick, Jain, Palmer, & Naeem, 2011) and is relevant for phyllosphere diversity
17
18 397 (Leff et al., 2018; Martínez-García, Richardson, Tylianakis, Peltzer, & Dickie, 2015; Yang et al.,
19
20 398 2019). Interestingly, we showed that leaf traits were mostly involved in shaping elevational
21
22 399 patterns of endophytic PMD, likely because they predominantly depend on the inner plant tissues
23
24 400 (Mina, Pereira, Lino-Neto, & Baptista, 2020; Yao et al., 2019). We further observed weak, but
25
26 401 significant indirect effects (up to 10%), highlighting that host plant traits are important biotic
27
28 402 drivers mediating climate effects on PMD. These indirect effects were 2-fold stronger for
29
30 403 endophytic than epiphytic communities, reinforcing the primary role of host plant traits in shaping
31
32 404 inner microbial communities. We acknowledge that our study did not consider interactive effects
33
34 405 between MAT and the biotic attributes of host plants, and it may have potentially underestimated
35
36 406 the strength of climate effects mediated by the local biotic filters. Our data also showed that the
37
38 407 effects of host plant traits were slightly stronger on phyllosphere fungal diversity than on bacterial
39
40 408 diversity. This result may arise from the higher transport material capacity of fungal mycelium
41
42 409 than that of bacteria (Boer et al., 2005; Jennings, 1987). While studies on mountain diversity
43
44 410 patterns yet barely considered fine-scale biotic filters, our results clearly highlight the need to
45
46 411 consider their direct and mediating effects to better understand plant–microbe associations and the
47
48 412 drivers shaping elevational diversity gradients.
49
50
51
52
53
54
55
56
57
58
59
60

1
2
3 413 The first axis of the PCA was positively related to leaf traits such as leaf area and SLA (and
4
5 414 negatively to LDMC; see Appendix Table S4). These leaf traits all belong to the Leaf Economic
6
7 415 Spectrum (Wright et al., 2004), one of the major axes of the global spectrum of plant forms and
8
9 416 functions (Diaz et al., 2016). They also represent influential plant functional attributes for
10
11 417 phyllosphere bacterial (LDMC and LA) and fungal (SLA) diversities (Kembel & Mueller, 2014).
12
13 418 Two main reasons could explain the importance of these functional attributes of host plants for
14
15 419 phyllosphere microbial diversity. First, they discriminate fast-growing acquisitive strategies and
16
17 420 resource uptake in plants (Kembel & Mueller, 2014), and thus relate to the plant's nutritional value
18
19 421 (Leveau, 2019; Liu, Brettell, & Singh, 2020 ; Vorholt, 2012). Second, traits such as LDMC have
20
21 422 been recently shown to relate to the leaf surface temperature (Liancourt, Song, Macek, Santrucek,
22
23 423 & Dolezal, 2020; Michaletz et al., 2015; Yang et al., 2021), a biophysical process involved in plant
24
25 424 species distribution along elevational gradients (Liancourt et al., 2020). As such, we may expect
26
27 425 that LDMC could also determine the bioclimate that PMD experience, and likely their distributions
28
29 426 along environmental gradients. While species-level trait measurements offer insights into PMD
30
31 427 patterns, we further advocate for incorporating intraspecific trait variation, a central component
32
33 428 influencing plant species interactions (Kraft, Crutsinger, Forrestel, & Emery, 2014; Le Bagousse-
34
35 429 Pinguet et al., 2015), and community assembly and dynamics (Bolnick et al., 2011; Violle et al.,
36
37 430 2012). Adopting an individual perspective of trait variation may further help to understand PMD
38
39 431 patterns, as well as to refine our predictions for community assembly, functional ecology and
40
41 432 plant–microbe associations.

42
43
44
45
46
47
48
49 433 Finally, we did not observe any covariation between bacteria and fungi, neither for endophytic
50
51 434 nor for epiphytic organisms, irrespective of the diversity metric considered (richness or Shannon's
52
53 435 diversity). Our result supports neutral associations between bacterial and fungal communities,
54
55
56
57
58
59
60

1
2
3 436 while we expected negative associations to occur as a signature of competition for space and
4
5 437 resources (Bahram et al., 2018). Two reasons may explain these results. On the one hand, the
6
7 438 absence of a relationship may highlight that stochastic assembly processes dominate as often
8
9 439 observed in other hyperdiverse systems such as the tropical forest biome (Harms, Condit, Hubbell,
10
11 440 & Foster, 2001). Neutral associations have been, for instance, observed in topsoil microbiomes,
12
13 441 particularly in agricultural systems (Jiao et al., 2021). On the other hand, neutral associations could
14
15 442 reflect the outcome of antagonistic deterministic processes fluctuating over time to shape microbial
16
17 443 communities (Götzenberger et al., 2012; Wang et al., 2016).
18
19
20
21
22 444

23 24 445 **Conclusions**

25
26 446 Our results offer the first step in understanding PMD associations and call for further investigation
27
28 447 to identify the putative underlying processing involved in shaping complex interactions among
29
30 448 microbial communities. We found a monotonous decline of phyllosphere microbial diversity with
31
32 449 increasing elevation, which contrasts with the commonly reported hump-shaped biodiversity
33
34 450 pattern along elevational gradients. Our work also demonstrated that host plant functional traits –
35
36 451 those involved in resource uptake and leaf surface temperature – predominantly shape endophytic
37
38 452 PMD patterns through both direct and indirect effects, while climate mostly impacted epiphytic
39
40 453 microbial communities. Our study provides a first hierarchical framework based on the simple
41
42 454 effect of traits to quantify the effects of biotic filters in shaping PMD patterns along ecological
43
44 455 gradients, and to disentangle their effects from those of the abiotic environment.
45
46
47
48

49 456 **Conflict of Interest Statement**

50
51 457 We ensure that none of the authors declared a conflict of interest.
52
53
54 458
55
56
57
58
59
60

459 **Author contributions**

460 ZY, XW and YLB-P conceived the idea; XW, ZY, FL, ZM, JY, SF, ZH and XW performed the
461 research and collected the data; XW, AA, ZY and YLB-P analysed the data; XW and YLB-P wrote
462 the first draft of the manuscript, and all of the authors contributed substantially to the revisions.

463

464 **Data Availability**

465 Microbe data are available from the NCBI Sequence Read Archive (SRA) database
466 (Accession Number: PRJNA824213), other data that support the findings of this study are
467 available from the corresponding author upon reasonable request.

468

469 **Acknowledgements**

470 This work was supported by the Strategic Priority Research Program of the Chinese Academy of
471 Sciences (XDA 23080301 & XDB 31030000), the National Natural Science Foundation of China
472 (32171581 , 31670632 , 31971439), the National Science Foundation of Liaoning Province of
473 China (2021-MS-028). AA is currently supported by Hebei University (Special Project No.
474 521100221033).

475

476 **Supporting Information**

477 **Fig. S1** Spearman correlations among candidate predictors (the abbreviations of leaf traits were
478 showed in Table S3)

479 **Fig. S2** Distribution of main phyla of phyllosphere microbes (the abbreviations of tree species
480 were shown in Table S1)

1
2
3
4
5
6
7
8
9
10
11
12
13
14
15
16
17
18
19
20
21
22
23
24
25
26
27
28
29
30
31
32
33
34
35
36
37
38
39
40
41
42
43
44
45
46
47
48
49
50
51
52
53
54
55
56
57
58
59
60

1
2
3 481 **Fig. S3** Relative abundances of the dominant phylum and class for bacterial and fungal in the
4
5 482 phyllosphere separated according to elevation categories. There were significant differences
6
7 483 between communities at different elevations. Abbreviations: Bacteria_{All}, all bacteria;
8
9 484 Bacteria_{Endo}, endophytic bacteria; Bacteria_{Epip}, epiphytic bacteria; Fungi_{All}, all fungi; Fungi_{Endo},
10
11 485 endophytic fungi; Fungi_{epip}, epiphytic fungi.

12
13
14 486 **Fig. S4** A conceptual model revealing the expected links of abiotic factors (mean annual
15
16 487 temperature) and biotic factors (leaf function traits) on phyllosphere microbial diversity.
17
18 488 Abbreviations: Bacteria_{All}, all bacteria; Bacteria_{Endo}, endophytic bacteria; Bacteria_{Epip}, epiphytic
19
20 489 bacteria; Fungi_{All}, all fungi; Fungi_{Endo}, endophytic fungi; Fungi_{epip}, epiphytic fungi.

21
22 490 **Fig. S5** Effects of mean annual temperature, plant identity(CWM_{MH}), and leaf functional traits
23
24 491 on phyllosphere bacterial (a, c, d) and fungal (b, e, f) Shannon's diversity. We present the
25
26 492 standardized regression coefficients of model predictors, and the associated 95% confidence
27
28 493 intervals. We also present the relative importance of each predictor (expressed as the percentage
29
30 494 of total variance). Significance levels are **: $P < 0.01$; ***: $P < 0.001$. Abbreviations: H,
31
32 495 Shannon's diversity; MAT, mean annual temperature; MAT², the square of mean annual
33
34 496 temperature; bacteria_{All}, all bacteria; Bacteria_{Endo}, endophytic bacteria; Bacteria_{Epip}, epiphytic
35
36 497 bacteria; Fungi_{All}, all fungi; Fungi_{Endo}, endophytic fungi; Fungi_{epip}, epiphytic fungi; CWM_{MH}, the
37
38 498 community-weighted mean of maximum tree height; FT_{PC1}, the first PCA axis on the nine
39
40 499 functional traits considered; FT_{PC2}, the second PCA axis.

41
42
43
44
45 500 **Figure. S6** Piecewise structural equation models (pSEMs) exploring the direct and indirect effects
46
47 501 of mean annual temperature and leaf functional traits on phyllosphere bacterial and fungi
48
49 502 Shannon's diversity. Standardized regression coefficients and significance are given (*<0.05,
50
51 503 **<0.01). The effect sizes of direct and indirect paths are also presented. Abbreviation: H,
52
53
54
55
56
57
58
59
60

1
2
3 504 Shannon's diversity; $Bacteria_{All}$, all bacteria; $Bacteria_{Endo}$, endophytic bacteria; $Bacteria_{Epip}$,
4 epiphytic bacteria; $Fungi_{All}$, all fungi; $Fungi_{Endo}$, endophytic fungi; $Fungi_{epip}$, epiphytic fungi; FT_{pc1} ,
5
6 505 the first PCA axis on the nine functional traits studied; MAT, mean annual temperature.
7
8
9

10
11 507 **Figure. S7** Piecewise structural equation models (pSEMs) exploring the effects of mean annual
12 temperature and leaf functional traits on phyllosphere bacterial and fungi richness. Standardized
13 regression coefficients and significance are given (* <0.05 , ** <0.01). Abbreviation: S, richness;
14
15 509 $Bacteria_{All}$, all bacteria; $Bacteria_{Endo}$, endophytic bacteria; $Bacteria_{Epip}$, epiphytic bacteria; $Fungi_{All}$,
16
17 510 all fungi; $Fungi_{Endo}$, endophytic fungi; $Fungi_{epip}$, epiphytic fungi; FT_{pc1} , the first PCA axis on the
18
19 511 nine functional traits studied; MAT, mean annual temperature.
20
21
22
23
24
25

26 513 **Figure. S8** Piecewise structural equation models (pSEMs) exploring the effects of mean annual
27 temperature and leaf functional traits on phyllosphere bacterial and fungi Shannon's diversity.
28 Standardized regression coefficients and significance are given (* <0.05 , ** <0.01). Abbreviation:
29
30 515 H, Shannon's diversity; $Bacteria_{All}$, all bacteria; $Bacteria_{Endo}$, endophytic bacteria; $Bacteria_{Epip}$,
31
32 516 epiphytic bacteria; $Fungi_{All}$, all fungi; $Fungi_{Endo}$, endophytic fungi; $Fungi_{epip}$, epiphytic fungi; FT_{pc1} ,
33
34 517 the first PCA axis on the nine functional traits studied; MAT, mean annual temperature.
35
36
37
38
39

40
41 519 **Figure. S9** Heatmap that shows relationship between plant functional traits and specific microbial
42 taxa (in the phyla level).
43
44

45 521
46
47 522 **Table S1** Summary of the main characteristics of sampling sites along an elevational gradient on
48 Changbai Mountain.
49

50 523
51
52 524 **Table S2** Geographic information of the studied sites.
53

54 525 **Table S3** Functional traits and their functions.
55
56
57
58
59
60

1
2
3 526 **Table S4** Loadings of the Principal Component Analysis for trait values.
4
5
6
7
8
9
10
11
12
13
14
15
16
17
18
19
20
21
22
23
24
25
26
27
28
29
30
31
32
33
34
35
36
37
38
39
40
41
42
43
44
45
46
47
48
49
50
51
52
53
54
55
56
57
58
59
60

For Peer Review

1
2
3
4 527 **Table S5** AIC value for predicting the relationship between phyllosphere microbial
5
6 528 richness and elevation(elevation²). Bold represents the optimal model based on AIC.
7
8
9 529 *: $P < 0.01$.

10
11 530 **Table S6** AIC value for predicting the relationship between phyllosphere microbial
12
13
14 531 Shannon index and elevation (elevation²). Bold represents the optimal model based on
15
16
17 532 AIC. *: $P < 0.01$.

18
19 533 **Table S7** The direct, indirect, and total standardized effects of mean annual
20
21
22 534 temperature and leaf functional traits on phyllosphere bacterial and fungal richness
23
24
25 535 derived from the pierce structural equation models. Models are presented in Fig. 4.
26
27 536 Only significant effects are shown.

28
29 537 **Table S8** The direct, indirect, and total standardized effects of mean annual
30
31
32 538 temperature and leaf functional traits on phyllosphere bacterial and fungal Shannon
33
34
35 539 index derived from the pierce structural equation models. Models are presented in Fig.
36
37 540 S5. Only significant effects are shown.

38
39
40 541 Figure legends

41
42
43 542 **Figure 1.** The geographical position of the Changbai Mountain in north-east China (a),
44
45 543 the location of study sites with the respective dominant forests (pictures) along an
46
47
48 544 elevational gradient from 800 m to 1950 m above sea level (b), and the design of the
49
50
51 545 study plot for samples collections (c).

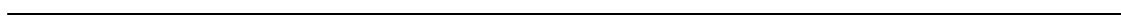
52
53 546 **Figure 2.** The richness of phyllosphere bacteria (a, b) and phyllosphere fungi (c, d)
54
55
56 547 along the studied elevational gradient. Abbreviations: S, richness; H, Shannon index;

1
2
3
4 548 Bacteria_{All}, all bacteria; Bacteria_{Endo}, endophytic bacteria; Bacteria_{Epip}, epiphytic
5
6 549 bacteria; Fungi_{All}, all fungi; Fungi_{Endo}, endophytic fungi; Fungi_{epip}, epiphytic fungi.
7
8
9

10 **Figure 3.** Effects of mean annual temperature, tree functional identity (CWM_{MH}), and
11
12 leaf functional traits on phyllosphere bacterial (a, c, d) and fungal (b, e, f) richness. We
13
14 present the standardized regression coefficients of model predictors and the associated
15
16 95% confidence intervals. We also present the relative importance of each predictor
17
18 (expressed as the percentage of total variance). Significance levels are **: $P < 0.01$;
19
20 ***: $P < 0.001$. Abbreviations: S, richness; MAT, mean annual temperature; MAT²,
21
22 the square of mean annual temperature; Bacteria_{All}, all bacteria; Bacteria_{Endo},
23
24 endophytic bacteria; Bacteria_{Epip}, epiphytic bacteria; Fungi_{All}, all fungi; Fungi_{Endo},
25
26 endophytic fungi; Fungi_{epip}, epiphytic fungi; FT_{PC1}, the first PCA axis on the nine
27
28 functional traits considered; FT_{PC2}, the second PCA axis.
29
30
31
32
33
34
35
36
37
38
39
40
41
42
43
44
45
46
47
48
49
50
51
52
53
54
55
56
57
58
59
60

561 **Figure 4.** Piecewise structural equation models (pSEMs) exploring the direct and
562
563 indirect effects of mean annual temperature and leaf functional traits on phyllosphere
564
565 bacterial and fungi richness. Standardized regression coefficients and significance are
566
567 given (* <0.05 , ** <0.01). The effect sizes of direct and indirect paths are also presented.
568
569 Abbreviation: S, richness; Bacteria_{All}, all bacteria; Bacteria_{Endo}, endophytic bacteria;
570
571 Bacteria_{Epip}, epiphytic bacteria; Fungi_{All}, all fungi; Fungi_{Endo}, endophytic fungi;
572
573 Fungi_{epip}, epiphytic fungi; FT_{pc1}, the first PCA axis on the nine functional traits studied;

1
2
3
4
5
6
7
8
9
10
11
12
13
14
15
16
17
18
19
20
21
22
23
24
25
26
27
28
29
30
31
32
33
34
35
36
37
38
39
40
41
42
43
44
45
46
47
48
49
50
51
52
53
54
55
56
57
58
59
60

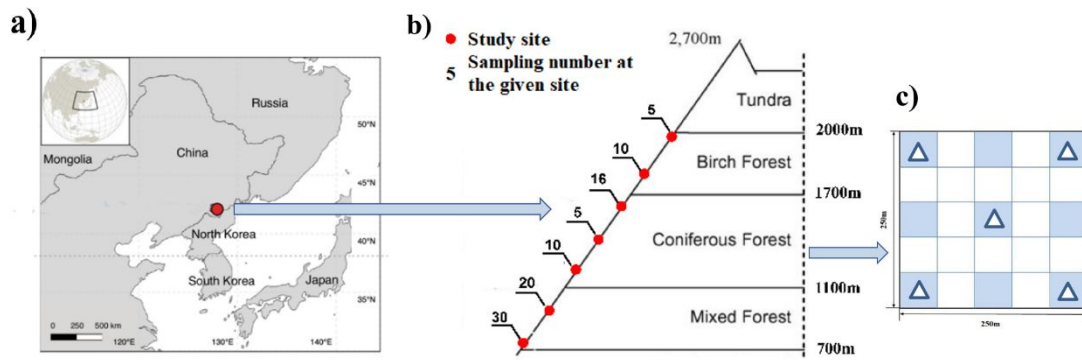


568 MAT, mean annual temperature.

569

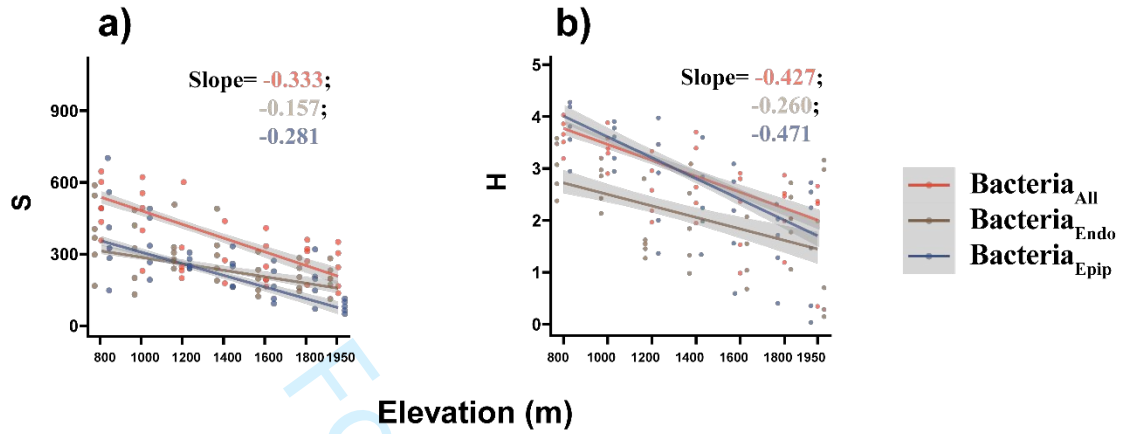
570

For Peer Review

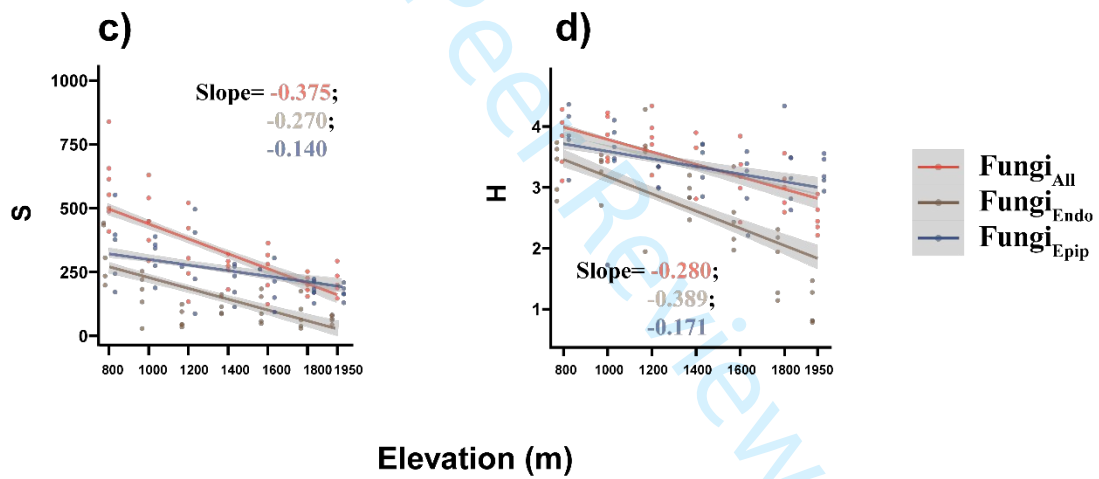
571 **Fig. 1**

575 Fig. 2

Bacteria



Fungi



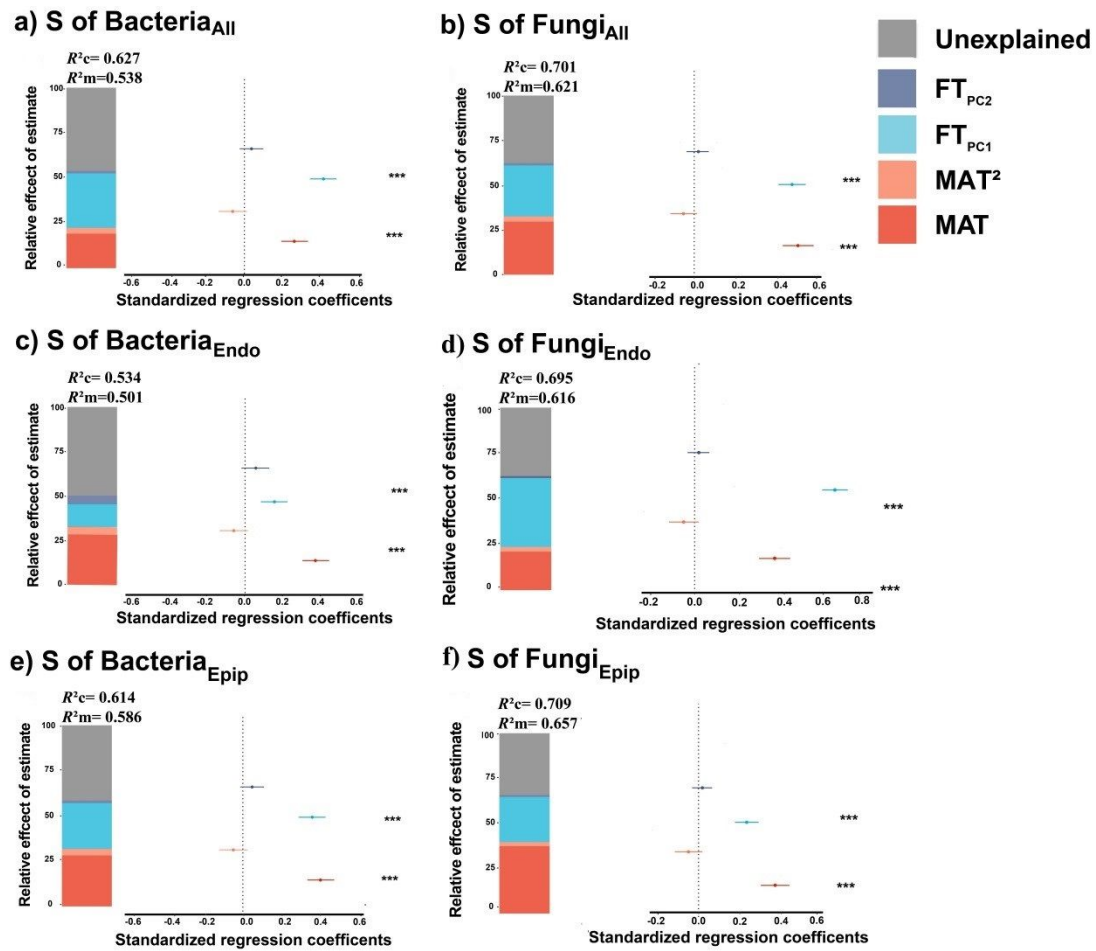
576

577

578

579

580 Fig. 3

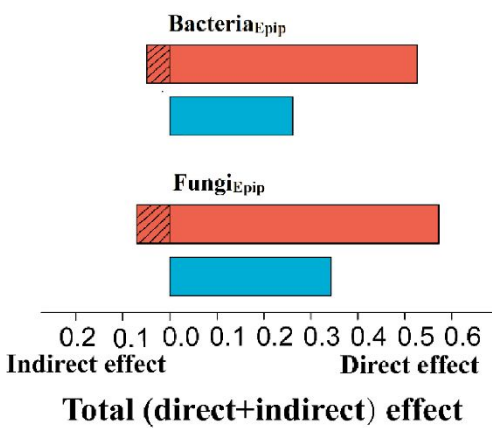
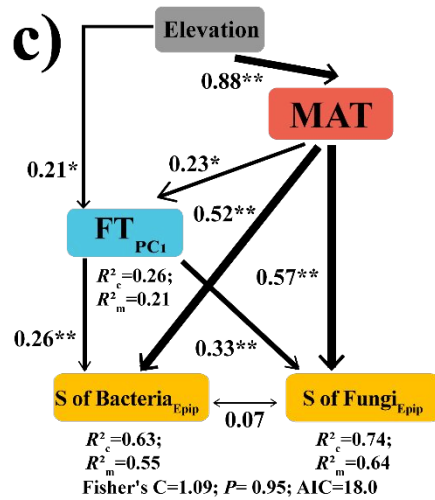
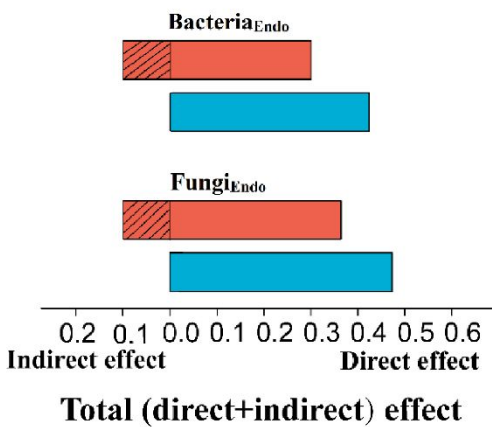
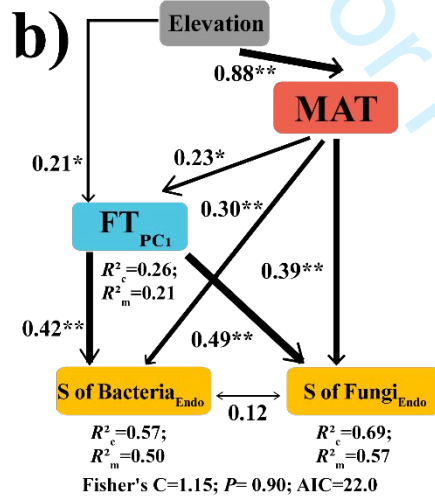
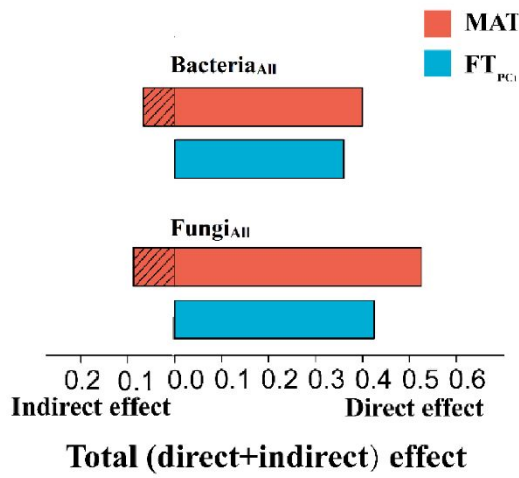
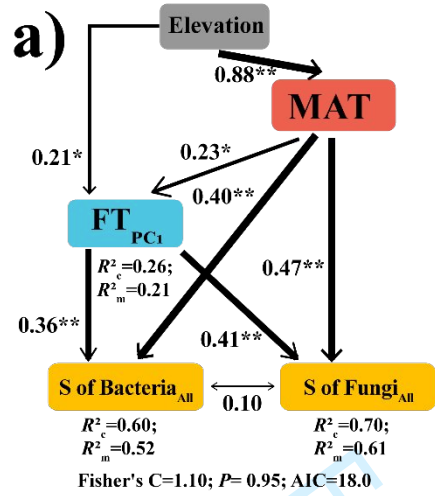


581

582

583

584 Fig. 4



585

586

587

588 References

- 589 Agler, M. T., Ruhe, J., Kroll, S., Morhenn, C., Kim, S. T., Weigel, D., & Kemen, E. M. (2016).
590 Microbial hub taxa link host and abiotic factors to plant microbiome variation. *Plos*
591 *Biology*, *14*(1), e1002352. doi:<https://doi.org/10.1371/journal.pbio.1002352>
- 592 Bahram, M., Hildebrand, F., Forslund, S., Anderson, J., Soudzilovskaia, N., Bodegom, P., . . .
593 Bork, P. (2018). Structure and function of the global topsoil microbiome. *Nature*, *560*,
594 233-237. doi:<https://doi.org/10.1038/s41586-018-0386-6>
- 595 Bartoń, K. (2020). MuMIn: Multi-model inference. *R package version 1.43.17*. [https://CRAN.R-](https://CRAN.R-project.org/package=MuMIn)
596 [project.org/package=MuMIn](https://CRAN.R-project.org/package=MuMIn).
- 597 Bodenhausen, N., Horton, M. W., & Bergelson, J. (2013). Bacterial communities associated
598 with the leaves and the roots of *Arabidopsis thaliana*. *Plos One*, *8*(2), e56329.
599 doi:<https://doi.org/10.1371/journal.pone.0056329>
- 600 Boer, W. d., Folman, L. B., Summerbell, R. C., & Boddy, L. (2005). Living in a fungal world:
601 impact of fungi on soil bacterial niche development. *FEMS Microbiology Reviews*, *29*(4),
602 795-811. doi:<https://doi.org/10.1016/j.femsre.2004.11.005>
- 603 Bolnick, D., Amarasekare, P., Araújo, M., Bürger, R., Levine, J., Novak, M., . . . Vasseur, D.
604 (2011). Why intraspecific trait variation matters in community ecology. *Trends in*
605 *Ecology and Evolution*, *26*, 183-192. doi:<https://doi.org/10.1016/j.tree.2011.01.009>
- 606 Brown, J. H., Gilgooly, J. F., Allen, A. P., Savage, V. M., & West, G. B. (2004). Toward a
607 metabolic theory of ecology. *Ecology*, *85*(7), 1771-1789. doi:
608 <https://doi.org/10.1890/03-9000>

- 1
2
3
4 609 Bruno, J. F., Stachowicz, J. J., & Bertness, M. D. (2003). Inclusion of facilitation into ecological
5
6 610 theory. *Trends in Ecology and Evolution*, *18*(3), 119-125.
7
8
9 611 doi:[https://doi.org/10.1016/S0169-5347\(02\)00045-9](https://doi.org/10.1016/S0169-5347(02)00045-9)
10
11
12 612 Bryant, J. A., Lamanna, C., Morlon, H., Kerkhoff, A. J., Enquist, B. J., & Green, J. L. (2008).
13
14 613 Microbes on mountainsides: Contrasting elevational patterns of bacterial and plant
15
16 614 diversity. *Proceedings of the National Academy of Sciences of the United States of*
17
18
19 615 *America*, *105*, 11505-11511. doi:<https://doi.org/10.1073/pnas.0801920105>
20
21
22 616 Bulgarelli, D., Garrido-Oter, R., Münch, P. C., Weiman, A., Dröge, J., Pan, Y., . . . microbe.
23
24 617 (2015). Structure and function of the bacterial root microbiota in wild and domesticated
25
26 618 barley. *Cell Host and Microbe*, *17*(3), 392-403.
27
28 619 doi:<https://doi.org/10.1016/j.chom.2015.01.011>
29
30
31 620 Bulgarelli, D., Rott, M., Schlaeppli, K., Ver Loren van Themaat, E., Ahmadinejad, N., Assenza,
32
33 621 F., . . . Schmelzer, E. (2012). Revealing structure and assembly cues for Arabidopsis
34
35 622 root-inhabiting bacterial microbiota. *Nature*, *488*(7409), 91-95.
36
37 623 doi:<https://doi.org/10.1038/nature11336>
38
39
40 624 Butterfield, B. J., Cavieres, L. A., Callaway, R. M., Cook, B. J., Kikvidze, Z., Lortie, C. J., . . .
41
42 625 Brooker, R. W. (2013). Alpine cushion plants inhibit the loss of phylogenetic diversity
43
44 626 in severe environments. *Ecol Lett*, *16*(4), 478-486.
45
46 627 doi:<https://doi.org/10.1111/ele.12070>
47
48
49 628 Carvalho, S. D., & Castillo, J. A. (2018). Influence of light on plant-phylosphere interaction.
50
51 629 *Frontiers in Plant Science*, *9*, 1482. doi:<https://doi.org/10.3389/fpls.2018.01482>
52
53
54
55
56
57
58
59
60

-
- 1
2
3
4 630 Cavieres, L. A., Brooker, R. W., Butterfield, B. J., Cook, B. J., Kikvidze, Z., Lortie, C. J., . . .
5
6 631 Callaway, R. M. (2014). Facilitative plant interactions and climate simultaneously drive
7
8
9 632 alpine plant diversity. *Ecol Lett*, *17*(2), 193-202. doi:<https://doi.org/10.1111/ele.12217>
10
11 633 Chave, J., Coomes, D., Jansen, S., Lewis, S. L., Swenson, N. G., & Zanne, A. E. (2009).
12
13
14 634 Towards a worldwide wood economics spectrum. *Ecol Lett*, *12*(4), 351-366.
15
16
17 635 doi:<https://doi.org/10.1111/j.1461-0248.2009.01285.x>
18
19 636 Cordier, T., Robin, C., Capdevielle, X., Olivier, F., Desprez-Loustau, M.-L., & Vacher, C. (2012).
20
21
22 637 The composition of phyllosphere fungal assemblages of European beech (*Fagus*
23
24 638 *sylvatica*) varies significantly along an elevation gradient. *New Phytologist*, *196*(2), 510-
25
26
27 639 519. doi:<https://doi.org/10.1111/j.1469-8137.2012.04284.x>
28
29 640 Devictor, V., Clavel, J., Julliard, R., Lavergne, S., Mouillot, D., Thuiller, W., . . . Mouquet, N.
30
31
32 641 (2010). Defining and measuring ecological specialization. *Journal of Applied Ecology*,
33
34 642 *47*(1), 15-25. doi:<https://doi.org/10.1111/j.1365-2664.2009.01744.x>
35
36
37 643 Diaz, S., Kattge, J., Cornelissen, J. H. C., Wright, I. J., Lavorel, S., Dray, S., . . . Gorne, L. D.
38
39
40 644 (2016). The global spectrum of plant form and function. *Nature*, *529*(7585), 167-171.
41
42
43 645 doi:<https://doi.org/10.1038/nature16489>
44
45 646 Díaz, S., Lavorel, S., de Bello, F., Quétier, F., Grigulis, K., & Robson, T. M. (2007). Incorporating
46
47
48 647 plant functional diversity effects in ecosystem service assessments. *Proceedings of the*
49
50
51 648 *National Academy of Sciences of the United States of America*, *104*(52), 20684-20689.
52
53 649 doi:<https://doi.org/10.1073/pnas.0704716104>
54
55 650 Duclos, T. R., DeLuca, W. V., & King, D. I. (2019). Direct and indirect effects of climate on bird
56
57
58
59
60

- 1
2
3
4 651 abundance along elevation gradients in the Northern Appalachian mountains. *Diversity*
5
6 652 *and Distributions*, 25(11), 1670-1683. doi:<https://doi.org/10.1111/ddi.12968>
7
8
9 653 Edgar, R. C. (2013). UPARSE: highly accurate OTU sequences from microbial amplicon reads.
10
11 654 *Nature Methods*, 10(10), 996-998. doi:<https://doi.org/10.1038/nmeth.2604>
12
13
14 655 Flynn, D. F., Mirochnick, N., Jain, M., Palmer, M. I., & Naeem, S. (2011). Functional and
15
16 656 phylogenetic diversity as predictors of biodiversity–ecosystem–function relationships.
17
18 657 *Ecology*, 92(8), 1573-1581. doi:<https://doi.org/10.1890/10-1245.1>
19
20
21 658 Geml, J., Arnold, A. E., Semenova-Nelsen, T. A., Nouhra, E. R., Drechsler-Santos, E. R., Goes-
22
23 659 Neto, A., . . . Lutzoni, F. (2022). Community dynamics of soil-borne fungal communities
24
25 660 along elevation gradients in neotropical and palaeotropical forests. *Molecular Ecology*,
26
27 661 31(7), 2044-2060. doi:<https://doi.org/10.1111/mec.16368>
28
29
30 662 Giangacomo, C., Mohseni, M., Kovar, L., & Wallace, J. G. (2021). Comparing DNA extraction
31
32 663 and 16S rRNA gene amplification methods for plant-associated bacterial communities.
33
34 664 *Phytobiomes Journal*, 5(2), 190-201. doi:[https://doi.org/10.1094/PBIOMES-07-20-](https://doi.org/10.1094/PBIOMES-07-20-0055-R)
35
36 665 [0055-R](https://doi.org/10.1094/PBIOMES-07-20-0055-R)
37
38
39 666 Gillooly, J. F., Brown, J. H., West, G. B., Savage, V. M., & Charnov, E. L. (2001). Effects of size
40
41 667 and temperature on metabolic rate. *Science*, 293(5538), 2248-2251.
42
43 668 doi:<https://doi.org/10.1126/science.1061967>
44
45
46 669 Gomes, T., Pereira, J., Benhadi-Marín, J., Lino-Neto, T., & Baptista, P. (2018). Endophytic and
47
48 670 epiphytic phyllosphere fungal communities are shaped by different environmental
49
50 671 factors in a Mediterranean ecosystem. *Microbial Ecology*, 76(3), 668-679.
51
52
53
54
55
56
57
58
59
60

- 1
2
3
4 672 [doi:https://doi.org/10.1007/s00248-018-1161-9](https://doi.org/10.1007/s00248-018-1161-9)
5
6
7 673 Götzenberger, L., de Bello, F., Bråthen, K. A., Davison, J., Dubuis, A., Guisan, A., . . . Zobel,
8
9 674 M. (2012). Ecological assembly rules in plant communities—approaches, patterns and
10
11 675 prospects. *Biological Reviews*, *87*(1), 111-127. doi:<https://doi.org/10.1111/j.1469->
12
13 676 [185X.2011.00187.x](https://doi.org/10.1111/j.1469-185X.2011.00187.x)
14
15
16
17 677 Graham, C. H., Parra, J. L., Rahbek, C., & McGuire, J. A. (2009). Phylogenetic structure in
18
19 678 tropical hummingbird communities. *Proceedings of the National Academy of Sciences*
20
21 *of the United States of America*, *106*, 19673-19678.
22
23 679 doi:<https://doi.org/10.1073/pnas.0901649106>
24
25 680
26
27 681 Gross, N., Börger, L., Morales, I., Le Bagousse-Pinguet, Y., Quero, J., Garcia-Gomez, M., . . .
28
29 682 Maestre, F. (2013). Uncovering multiscale effects of aridity and biotic interactions on
30
31 683 the functional structure of Mediterranean shrubland. *Journal of Ecology*, *101*, 637-649.
32
33 684 doi:<https://doi.org/10.1111/1365-2745.12063>
34
35
36
37 685 Grytnes, J. A., & Beaman, J. H. (2006). Elevational species richness patterns for vascular plants
38
39 686 on Mount Kinabalu, Borneo. *Journal Of Biogeography*, *33*(10), 1838-1849.
40
41 687 doi:<https://doi.org/10.1111/j.1365-2699.2006.01554.x>
42
43
44
45 688 Guo, Q., Kelt, D., Sun, Z., Liu, H., Hu, L., Ren, H., & Wen, J. (2013). Global variation in
46
47 689 elevational diversity patterns. *Scientific Reports*, *3*, 3007.
48
49 690 doi:<https://doi.org/10.1038/srep03007>
50
51
52
53 691 Harms, K., Condit, R., Hubbell, S., & Foster, R. (2001). Habitat associations of trees and shrubs
54
55 692 in a 50-ha Neotropical forest plot. *Journal of Ecology*, *89*, 947-959.
56
57
58
59
60

- 1
2
3
4 693 doi:<https://doi.org/10.1046/j.0022-0477.2001.00615.x>
5
6 694 Herrmann, M., Geesink, P., Richter, R., & Küsel, K. (2021). Canopy position has a stronger
7
8 695 effect than tree species identity on phyllosphere bacterial diversity in a floodplain
9
10
11 696 hardwood forest. *Microbial Ecology*, 81(1), 157-168.
12
13 697 doi:<https://doi.org/10.1007/s00248-020-01565-y>
14
15
16 698 Inácio, J., Pereira, P., Carvalho, d. M., Fonseca, A., Amaral-Collaco, M., & Spencer-Martins, I.
17
18 699 (2002). Estimation and diversity of phylloplane mycobiota on selected plants in a
19
20 700 mediterranean-type ecosystem in Portugal. *Microbial Ecology*, 44(4), 344-353.
21
22
23 701 Jennings, D. (1987). Translocation of solutes in fungi. *Biological Reviews*, 62(3), 215-243.
24
25 702 doi:<https://doi.org/10.1111/j.1469-185X.1987.tb00664.x>
26
27
28 703 Jia, T., Yao, Y., Guo, T., Wang, R., & Chai, B. (2020). Effects of plant and soil characteristics
29
30 704 on phyllosphere and rhizosphere fungal communities during plant development.
31
32 705 *Frontiers in Microbiology*, 11, doi: 10.3389/fmicb.2020.556002.
33
34 706 doi:<https://doi.org/10.3389/fmicb.2020.556002>
35
36
37 707 Jiao, S., Peng, Z., Qi, J., Gao, J., Wei, G., & Stegen, J. C. (2021). Linking bacterial-fungal
38
39 708 relationships to microbial diversity and soil nutrient cycling. *Msystems*, 6(2), e01052-
40
41 709 01020. doi:<https://doi.org/10.1128/mSystems.01052-20>
42
43
44 710 Kembel, S. W., & Mueller, R. C. (2014). Plant traits and taxonomy drive host associations in
45
46 711 tropical phyllosphere fungal communities. *Botany*, 92(4), 1-10.
47
48 712 doi:<https://doi.org/10.1139/cjb-2013-0194>
49
50
51 713 Kembel, S. W., O'Connor, T. K., Arnold, H. K., Hubbell, S. P., Wright, S. J., & Green, J. L.
52
53
54
55
56
57
58
59
60

- 1
2
3
4 714 (2014). Relationships between phyllosphere bacterial communities and plant functional
5
6 715 traits in a neotropical forest. *Proceedings of the National Academy of Sciences of the*
7
8
9 716 *United States of America*, 111(38), 13715-13720.
10
11 717 doi:<https://doi.org/10.1073/pnas.1216057111>
12
13
14 718 Körner, C. (2000). Why are there global gradients in species richness? Mountains might hold
15
16 719 the answer. *Trends in Ecology and Evolution*, 15, 513-514.
17
18
19 720 doi:[https://doi.org/10.1016/S0169-5347\(00\)02004-8](https://doi.org/10.1016/S0169-5347(00)02004-8)
20
21
22 721 Kotilinek, M., Hiiesalu, I., Kosnar, J., Smilauerov, M., Smilauer, P., Altman, J., . . . Dolezal, J.
23
24 722 (2017). Fungal root symbionts of high-altitude vascular plants in the Himalayas.
25
26 723 *Scientific Reports*, 7, 1-14. doi:<https://doi.org/10.1038/s41598-017-06938-x>
27
28
29 724 Kraft, N., Crutsinger, G., Forrestel, E., & Emery, N. (2014). Functional trait differences and the
30
31 725 outcome of community assembly: An experimental test with vernal pool annual plants.
32
33 726 *Oikos*, 123(11), 1391-1399. doi:<https://doi.org/10.1111/oik.01311>
34
35
36 727 Le Bagousse-Pinguet, Y., Börger, L., Quero, J., García-Gómez, M., Soriano, S., Maestre, F., &
37
38 728 Gross, N. (2015). Traits of neighbouring plants and space limitation determine
39
40 729 intraspecific trait variability in semi-arid shrublands. *Journal of Ecology*, 103(6), 1647-
41
42 730 1657. doi:<https://doi.org/10.1111/1365-2745.12480>
43
44
45 731 Le Bagousse-Pinguet, Y., Gross, N., Maestre, F. T., Maire, V., de Bello, F., Fonseca, C. R., . . .
46
47 732 Liancourt, P. (2017). Testing the environmental filtering concept in global drylands.
48
49 733 *Journal of Ecology*, 105(4), 1058-1069. doi:<https://doi.org/10.1111/1365-2745.12735>
50
51
52 734 Le Bagousse-Pinguet, Y., Liancourt, P., Götzenberger, L., de Bello, F., Altman, J., Brozova, V.,
53
54
55
56
57
58
59
60

- 1
2
3
4 735 . . . Dolezal, J. (2018). A multi-scale approach reveals random phylogenetic patterns at
5
6 736 the edge of vascular plant life. *Perspectives in Plant Ecology, Evolution and*
7
8
9 737 *Systematics*, 30, 22-30. doi:<https://doi.org/10.1016/j.ppees.2017.https://doi.org/10.002>
10
11 738 Le Bagousse-Pinguet, Y., Soliveres, S., Gross, N., Torices, R., Berdugo, M., & Maestre, F. T.
12
13
14 739 (2019). Phylogenetic, functional, and taxonomic richness have both positive and
15
16
17 740 negative effects on ecosystem multifunctionality. *Proceedings of the National Academy*
18
19 741 *of Sciences of the United States of America*, 116(17), 8419-8424.
20
21
22 742 doi:<https://doi.org/10.1073/pnas.1815727116>
23
24
25 743 Lefcheck, J. S. (2016). PIECEWISESEM: Piecewise structural equation modelling in R for
26
27 744 ecology, evolution, and systematics. *Methods in Ecology and Evolution*, 7(5), 573-579.
28
29
30 745 doi:<https://doi.org/10.1111/2041-210x.12512>
31
32
33 746 Leff, J., Bardgett, R., Wilkinson, A., Jackson, B., Pritchard, W., De Long, J., . . . Fierer, N. (2018).
34
35 747 Predicting the structure of soil communities from plant community taxonomy,
36
37 748 phylogeny, and traits. *The ISME journal*, 12(7), 1794-1805.
38
39
40 749 doi:<https://doi.org/10.1038/s41396-018-0089-x>
41
42
43 750 Leveau, J. H. J. (2019). A brief from the leaf: latest research to inform our understanding of the
44
45 751 phyllosphere microbiome. *Current Opinion in Microbiology*, 49, 41-49.
46
47
48 752 doi:<https://doi.org/10.1016/j.mib.2019.https://doi.org/10.002>
49
50
51 753 Liancourt, P., Song, X., Macek, M., Santrucek, J., & Dolezal, J. (2020). Plant's-eye view of
52
53 754 temperature governs elevational distributions. *Global Change Biology*, 26(7), 4094-
54
55
56 755 4103. doi:<https://doi.org/10.1111/gcb.15129>
57
58
59
60

- 1
2
3
4 756 Liu, H., Brettell, L. E., & Singh, B. (2020). Linking the phyllosphere microbiome to plant health.
5
6 757 *Trends in Plant Science*, 25(9), 841-844.
7
8
9 758 doi:<https://doi.org/10.1016/j.tplants.2020.06.003>
10
11 759 Lundberg, D. S., Lebeis, S. L., Paredes, S. H., Yourstone, S., Gehring, J., Malfatti, S., . . . Rio,
12
13
14 760 T. G. d. (2012). Defining the core *Arabidopsis thaliana* root microbiome. *Nature*,
15
16 761 488(7409), 86-90. doi:<https://doi.org/10.1038/nature11237>
17
18
19 762 Machac, A., Janda, M., Dunn, R. R., & Sanders, N. J. (2011). Elevational gradients in
20
21 763 phylogenetic structure of ant communities reveal the interplay of biotic and abiotic
22
23 764 constraints on diversity. *Ecography*, 34(3), 364-371. doi:<https://doi.org/10.1111/j.1600->
24
25 765 [0587.2010.06629.x](https://doi.org/10.1111/j.1600-0587.2010.06629.x)
26
27
28
29 766 Mao, Z., Corrales, A., Zhu, K., Yuan, Z., Lin, F., Ye, J., . . . Wang, X. (2019). Tree mycorrhizal
30
31 767 associations mediate soil fertility effects on forest community structure in a temperate
32
33 768 forest. *New Phytologist*, 223(1), 475-486. doi:<https://doi.org/10.1111/nph.15742>
34
35
36
37 769 Martínez-García, L. B., Richardson, S. J., Tylianakis, J. M., Peltzer, D. A., & Dickie, I. A. (2015).
38
39 770 Host identity is a dominant driver of mycorrhizal fungal community composition during
40
41 771 ecosystem development. *New Phytologist*, 205(4), 1565-1576.
42
43
44
45 772 Michaletz, S. T., Weiser, M. D., Zhou, J., Kaspari, M., Helliker, B. R., & Enquist, B. J. (2015).
46
47 773 Plant thermoregulation: energetics, trait-environment interactions, and carbon
48
49 774 economics. *Trends in Ecology and Evolution*, 30(12), 714-724.
50
51 775 doi:<https://doi.org/10.1016/j.tree.2015.09.006>
52
53
54
55 776 Mina, D., Pereira, J., Lino-Neto, T., & Baptista, P. (2020). Epiphytic and endophytic bacteria on
56
57
58
59
60

- 1
2
3
4 777 olive tree phyllosphere: exploring tissue and cultivar effect. *Microbial Ecology*, 80, 145–
5
6 778 157. doi:<https://doi.org/10.1007/s00248-020-01488-8>
7
8
9 779 Nottingham, A. T., Fierer, N., Turner, B. L., Whitaker, J., Ostle, N. J., McNamara, N. P., . . .
10
11 780 Meir, P. (2018). Microbes follow Humboldt: temperature drives plant and soil microbial
12
13 781 diversity patterns from the Amazon to the Andes. *Ecology*, 99(11), 2455-2466.
14
15 782 doi:<https://doi.org/10.1002/ecy.2482>
16
17
18
19 783 Pérez-Harguindeguy, N., Díaz, S., Garnier, E., Lavorel, S., Poorter, H., Jaureguiberry, P., . . .
20
21 784 Gurvich, D. (2013). New handbook for standardised measurement of plant functional
22
23 785 traits worldwide. *Australian Journal of botany*, 61(3), 167-234.
24
25
26
27 786 Rahbek, C. (1995). The elevational gradient of species richness: a uniform pattern? *Ecography*,
28
29 787 18(2), 200-205.
30
31
32 788 Rahbek, C., Borregaard, M. K., Colwell, R. K., Dalsgaard, B., Holt, B. G., Morueta-Holme, N., .
33
34 . . . Fjeldså, J. (2019). Humboldt's enigma: What causes global patterns of mountain
35
36 789 biodiversity? *Science*, 365(6458), 1108-1113.
37
38 790 doi:<https://doi.org/10.1126/science.aax0149>
39
40
41
42 792 Rehakova, K., Chlumská, Z., & Doležal, J. (2011). Soil cyanobacterial and microalgal diversity
43
44 793 in dry mountains of Ladakh, NW Himalaya, as related to site, altitude, and vegetation.
45
46 794 *Microbial Ecology*, 62(2), 337-346. doi:<https://doi.org/10.1007/s00248-011-9878-8>
47
48
49
50 795 Sanders, N. J. (2002). Elevational gradients in ant species richness: area, geometry, and
51
52 796 Rapoport's rule. *Ecography*, 25(1), 25-32. doi:<https://doi.org/10.1034/j.1600-0587.2002.250104.x>
53
54
55
56
57
58
59
60

- 1
2
3
4 798 Shao, G., Schall, P., & Weishampel, J. F. (1994). Dynamic simulations of mixed broadleaved-
5
6 799 Pinus koraiensis forests in the Changbaishan Biosphere Reserve of China. *Forest*
7
8
9 800 *Ecology and Management*, 70(1-3), 169-181.
- 10
11 801 Shen, C., Liang, W., Shi, Y., Lin, X., Zhang, H., Wu, X., . . . Chu, H. (2014). Contrasting
12
13 802 elevational diversity patterns between eukaryotic soil microbes and plants. *Ecology*,
14
15 803 95(11), 3190-3202. doi:<https://doi.org/10.1890/14-0310.1>
- 16
17 804 Shen, C., Xiong, J., Zhang, H., Feng, Y., Lin, X., Li, X., . . . Chu, H. (2013). Soil pH drives the
18
19 805 spatial distribution of bacterial communities along elevation on Changbai Mountain.
20
21 806 *Soil Biology and Biochemistry*, 57, 204-211.
22
23 807 doi:<https://doi.org/10.1016/j.soilbio.2012.07.013>
- 24
25 808 Shipley, B. (2009). Confirmatory path analysis in a generalized multilevel context. *Ecology*,
26
27 809 90(2), 363-368. doi:<https://doi.org/10.1890/08-1034.1>
- 28
29 810 Shrestha, N., Su, X., Xu, X., & Wang, Z. (2018). The drivers of high *Rhododendron* diversity in
30
31 811 south-west China: Does seasonality matter? *Journal Of Biogeography*, 45(2), 438-447.
32
33 812 doi:<https://doi.org/10.1111/jbi.13136>
- 34
35 813 Smith, M. A., Hallwachs, W., & Janzen, D. H. (2014). Diversity and phylogenetic community
36
37 814 structure of ants along a Costa Rican elevational gradient. *Ecography*, 37(8), 720-731.
38
39 815 doi:<https://doi.org/10.1111/j.1600-0587.2013.00631.x>
- 40
41 816 Stone, R. (2006). A threatened nature reserve breaks down Asian borders. *Science*, 313(5792),
42
43 817 1379-1380. doi:<https://doi.org/10.1126/science.313.5792.1379>
- 44
45 818 Vacher, C., Cordier, T., & Vallance, J. (2016). Phyllosphere fungal communities differentiate
46
47
48
49
50
51
52
53
54
55
56
57
58
59
60

- 1
2
3
4 819 more thoroughly than bacterial communities along an elevation gradient. *Microbial*
5
6 820 *Ecology*, 72(1), 1-3. doi:<https://doi.org/10.1007/s00248-016-0742-8>
7
8
9 821 Vacher, C., Hampe, A., Porté, A. J., Sauer, U., Compant, S., & Morris, C. E. (2016). The
10
11 822 phyllosphere: Microbial jungle at the plant-climate interface. *Annual Review of Ecology,*
12
13 823 *Evolution, and Systematics*, 47(1), 1-24. doi:[https://doi.org/10.1146/annurev-ecolsys-](https://doi.org/10.1146/annurev-ecolsys-121415-032238)
14
15 824 [121415-032238](https://doi.org/10.1146/annurev-ecolsys-121415-032238)
16
17
18
19 825 Violle, C., Enquist, B., McGill, B., Jiang, L., Albert, C., Hulshof, C., . . . Messier, J. (2012). The
20
21 826 return of the variance: Intraspecific variability in community ecology. *Trends in Ecology*
22
23 827 *and Evolution*, 27, 244-252. doi:<https://doi.org/10.1016/j.tree.2011.11.014>
24
25
26
27 828 Von Humboldt, A., & Bonpland, A. (1805). Essai sur la géographie des plantes (Chez Levrault,
28
29 829 Schoell et compagnie, libraires, Paris).
30
31
32 830 Vorholt, J. A. (2012). Microbial life in the phyllosphere. *Nature Reviews Microbiology*, 10(12),
33
34 831 828-840. doi:<https://doi.org/10.1038/nrmicro2910>
35
36
37
38 832 Wang, F., Harindintwali, J. D., Yuan, Z., Min, W., Wang, F., Li, S., . . . Chen, J. (2021).
39
40 833 Technologies and perspectives for achieving carbon neutrality. *The Innovation*, 2(4),
41
42 834 100-180. doi:<https://doi.org/10.1016/j.xinn.2021.100180>
43
44
45
46 835 Wang, J., Meier, S., Soininen, J., Casamayor, E. O., Pan, F., Tang, X., . . . Shen, J. (2017).
47
48 836 Regional and global elevational patterns of microbial species richness and evenness.
49
50 837 *Ecology*, 98(3), 393-402. doi:<https://doi.org/10.1111/ecog.02216>
51
52
53
54 838 Wang, Q., Garrity, G. M., Tiedje, J. M., & Cole, J. R. (2007). Naive Bayesian classifier for rapid
55
56 839 assignment of rRNA sequences into the new bacterial taxonomy. *Applied and*

- 1
2
3
4 840 *Environmental Microbiology* 73(16), 5261-5267.
5
6 841 doi:<https://doi.org/10.1128/aem.00062-07>
7
8
9 842 Wang, X., Swenson, N. G., Wiegand, T., Wolf, A., Howe, R., Lin, F., . . . Bai, X. (2013).
10
11 843 Phylogenetic and functional diversity area relationships in two temperate forests.
12
13 844 *Ecography*, 36(8), 883-893. doi:<https://doi.org/10.1111/j.1600-0587.2012.00011.x>
14
15
16
17 845 Wang, X., Wiegand, T., Kraft, N. J., Swenson, N. G., Davies, S. J., Hao, Z., . . . Mi, X. (2016).
18
19 846 Stochastic dilution effects weaken deterministic effects of niche-based processes in
20
21 847 species rich forests. *Ecology*, 97(2), 347-360. doi:<https://doi.org/10.1890/14-2357.1>
22
23
24
25 848 Wei, T., Simko, V., Levy, M., Xie, Y., Jin, Y., & Zemla, J. (2017). Package ‘corrplot’. *Statistician*,
26
27 849 56(316), e24.
28
29
30 850 Wei, Y., Lan, G., Wu, Z., Chen, B., Quan, F., Li, M., . . . Du, H. (2022). Phyllosphere fungal
31
32 851 communities of rubber trees exhibited biogeographical patterns, but not bacteria.
33
34 852 *Environmental microbiology*, 24, 3777-3790. doi:[https://doi.org/10.1111/1462-](https://doi.org/10.1111/1462-2920.15894)
35
36 853 [2920.15894](https://doi.org/10.1111/1462-2920.15894)
37
38
39
40 854 Weiher, E., Clarke, G. D. P., & Keddy, P. A. (1998). Community assembly rules, morphological
41
42 855 dispersion, and the coexistence of plant species. *Oikos*, 81(2), 309-322.
43
44 856 doi:<https://doi.org/10.2307/3547051>
45
46
47
48 857 Wright, I., Reich, P., Westoby, M., Ackerly, D., Baruch, Z., Bongers, F., . . . Villar, R. (2004).
49
50 858 The world-wide leaf economics spectrum. *Nature*, 21(428), 821-827.
51
52 859 doi:<https://doi.org/10.1111/j.1466-8238.2012.00761.x>
53
54
55
56 860 Yang, H. (1985). Distribution patterns of dominant tree species on northern slope of Changbai
57
58
59
60

- 1
2
3
4 861 Mountain. *Research Forest Ecosystem*, 5, 1-14.
- 5
6 862 Yang, T., Tedersoo, L., Soltis, P., Soltis, D., Gilbert, J., Sun, M., . . . Chu, H. (2019).
7
8
9 863 Phylogenetic imprint of woody plants on the soil mycobiome in natural mountain forests
10
11 864 of eastern China. *The ISME journal*, 13, 686-697. doi:[https://doi.org/10.1038/s41396-](https://doi.org/10.1038/s41396-018-0303-x)
12
13
14 865 [018-0303-x](https://doi.org/10.1038/s41396-018-0303-x)
- 15
16
17 866 Yang, X., Wu, J., Chen, X., Ciais, P., Maignan, F., Yuan, W., . . . Wright, S. J. (2021). A
18
19 867 comprehensive framework for seasonal controls of leaf abscission and productivity in
20
21 868 evergreen, broadleaved tropical and subtropical forests. *The Innovation*, 2, 100154.
22
23
24 869 doi:<https://doi.org/10.1016/j.xinn.2021.100154>
- 25
26
27 870 Yao, H., Sun, X., He, C., Li, X.-C., & Guo, L.-D. (2020). Host identity is more important in
28
29 871 structuring bacterial epiphytes than endophytes in a tropical mangrove forest. *Fems*
30
31 872 *Microbiology Ecology*, 96(4), fiae038. doi:<https://doi.org/10.1093/femsec/fiae038>
- 32
33
34 873 Yao, H., Sun, X., He, C., Maitra, P., Li, X.-C., & Guo, L.-D. (2019). Phyllosphere epiphytic and
35
36 874 endophytic fungal community and network structures differ in a tropical mangrove
37
38 875 ecosystem. *Microbiome*, 7(1), 1-15. doi:<https://doi.org/10.1186/s40168-019-0671-0>
- 39
40
41
42 876 Yuan, Z., Ali, A., Loreau, M., Ding, F., Liu, S., Sanaei, A., . . . Le Bagousse-Pinguet, Y. (2021).
43
44 877 Divergent above- and below-ground biodiversity pathways mediate disturbance
45
46 878 impacts on temperate forest multifunctionality. *Global Change Biology*, 27(12), 2883-
47
48 879 2894. doi:<https://doi.org/10.1111/gcb.15606>
- 49
50
51
52 880 Yuan, Z., Ali, A., Ruiz-Benito, P., Jucker, T., Mori, A., Wang, S., . . . Loreau, M. (2020). Above
53
54 881 - and below-ground biodiversity jointly regulate temperate forest multifunctionality

1
2
3
4 882 along a local -scale environmental gradient. *Journal of Ecology*, 108, 2012– 2024.

5
6 883 doi:<https://doi.org/10.1111/1365-2745.13378>

7
8
9 884 Yuan, Z., Gazol, A., Lin, F., Ye, J., Shi, S., Wang, X., . . . Hao, Z. (2013). Soil organic carbon

10
11 885 in an old-growth temperate forest: spatial pattern, determinants and bias in its

12
13
14 886 quantification. *Geoderma*, 195, 48-55.

15
16 887 doi:<https://doi.org/10.1016/j.geoderma.2012.11.008>

17
18
19 888 Zhang, J.-T., Xiao, J., & Li, L. (2015). Variation of plant functional diversity along a disturbance

20
21 889 gradient in mountain meadows of the Donglingshan reserve, Beijing, China. *Russian*

22
23
24 890 *Journal of Ecology*, 46(2), 157-166. doi:<https://doi.org/10.1134/s1067413615020058>

25
26
27 891 Zhao, W. L., Chen, Y. J., Brodribb, T. J., & Cao, K. F. (2016). Weak co-ordination between vein

28
29 892 and stomatal densities in 105 angiosperm tree species along altitudinal gradients in

30
31
32 893 Southwest China. *Functional Plant Biology*, 43(12), 1126-1133.

33
34 894 doi:<https://doi.org/10.1071/fp16012>

35
36
37 895 Zhu, Y. G., Xiong, C., Wei, Z., Chen, Q. L., Ma, B., Zhou, S. Y. D., . . . Duan, G. L. J. N. P.

38
39 896 (2021). Impacts of global change on phyllosphere microbiome. *New Phytologist*, 234,

40
41
42 897 1977-1986. doi:<https://doi.org/10.1111/nph.17928>

43
44
45 898

Supporting information

Fig. S1 Spearman correlations among candidate predictors (the abbreviations of leaf traits were showed in Table S3)

Fig. S2 Distribution of main phyla of phyllosphere microbes (the abbreviations of tree species were shown in Table S1)

Fig. S3 Relative abundances of the dominant phylum and class for bacterial and fungal in the phyllosphere separated according to elevation categories. There were significant differences between communities at different elevations. Abbreviations: Bacteria_{All}, all bacteria; Bacteria_{Endo}, endophytic bacteria; Bacteria_{Epip}, epiphytic bacteria; Fungi_{All}, all fungi; Fungi_{Endo}, endophytic fungi; Fungi_{epip}, epiphytic fungi.

Fig. S4 A conceptual model revealing the expected links of abiotic factors (mean annual temperature) and biotic factors (leaf function traits) on phyllosphere microbial diversity.

Abbreviations: Bacteria_{All}, all bacteria; Bacteria_{Endo}, endophytic bacteria; Bacteria_{Epip}, epiphytic bacteria; Fungi_{All}, all fungi; Fungi_{Endo}, endophytic fungi; Fungi_{epip}, epiphytic fungi.

Fig. S5 Effects of mean annual temperature, plant identity(CWM_{MH}), and leaf functional traits on phyllosphere bacterial (a, c, d) and fungal (b, e, f) Shannon's diversity. We present the standardized regression coefficients of model predictors, and the associated 95% confidence intervals. We also present the relative importance of each predictor (expressed as the percentage of total variance). Significance levels are **: $P < 0.01$; ***: $P < 0.001$. Abbreviations: H, Shannon's diversity; MAT, mean annual temperature; MAT², the square of mean annual temperature; bacteria_{All}, all bacteria; Bacteria_{Endo}, endophytic bacteria; Bacteria_{Epip}, epiphytic bacteria; Fungi_{All}, all fungi; Fungi_{Endo}, endophytic fungi; Fungi_{epip}, epiphytic fungi; CWM_{MH}, the

1
2
3 community-weighted mean of maximum tree height; FT_{PC1} , the first PCA axis on the nine
4
5 functional traits considered; FT_{PC2} , the second PCA axis.
6
7

8
9 **Figure. S6** Piecewise structural equation models (pSEMs) exploring the direct and indirect effects
10
11 of mean annual temperature and leaf functional traits on phyllosphere bacterial and fungi
12
13 Shannon's diversity. Standardized regression coefficients and significance are given ($* < 0.05$,
14
15 $** < 0.01$). The effect sizes of direct and indirect paths are also presented. Abbreviation: H,
16
17 Shannon's diversity; $Bacteria_{All}$, all bacteria; $Bacteria_{Endo}$, endophytic bacteria; $Bacteria_{Epip}$,
18
19 epiphytic bacteria; $Fungi_{All}$, all fungi; $Fungi_{Endo}$, endophytic fungi; $Fungi_{epip}$, epiphytic fungi; FT_{pc1} ,
20
21 the first PCA axis on the nine functional traits studied; MAT, mean annual temperature.
22
23
24
25

26
27 **Figure. S7** Piecewise structural equation models (pSEMs) exploring the effects of mean annual
28
29 temperature and leaf functional traits on phyllosphere bacterial and fungi richness. Standardized
30
31 regression coefficients and significance are given ($* < 0.05$, $** < 0.01$). Abbreviation: S, richness;
32
33 $Bacteria_{All}$, all bacteria; $Bacteria_{Endo}$, endophytic bacteria; $Bacteria_{Epip}$, epiphytic bacteria; $Fungi_{All}$,
34
35 all fungi; $Fungi_{Endo}$, endophytic fungi; $Fungi_{epip}$, epiphytic fungi; FT_{pc1} , the first PCA axis on the
36
37 nine functional traits studied; MAT, mean annual temperature.
38
39
40

41
42 **Figure. S8** Piecewise structural equation models (pSEMs) exploring the effects of mean annual
43
44 temperature and leaf functional traits on phyllosphere bacterial and fungi Shannon's diversity.
45
46 Standardized regression coefficients and significance are given ($* < 0.05$, $** < 0.01$). Abbreviation:
47
48 H, Shannon's diversity; $Bacteria_{All}$, all bacteria; $Bacteria_{Endo}$, endophytic bacteria; $Bacteria_{Epip}$,
49
50 epiphytic bacteria; $Fungi_{All}$, all fungi; $Fungi_{Endo}$, endophytic fungi; $Fungi_{epip}$, epiphytic fungi; FT_{pc1} ,
51
52 the first PCA axis on the nine functional traits studied; MAT, mean annual temperature.
53
54

55
56 **Figure. S9** Heatmap that shows relationship between plant functional traits and specific microbial
57
58
59
60

1
2
3 taxa (in the phyla level).
4
5
6
7

8 **Table S1** Summary of the main characteristics of sampling sites along an elevational gradient on
9 Changbai Mountain.
10

11 **Table S2** Geographic information of the studied sites.
12

13 **Table S3** Functional traits and their functions.
14

15 **Table S4** Loadings of the Principal Component Analysis for trait values.
16

17 **Table S5** AIC value for predicting the relationship between phyllosphere microbial richness and
18 elevation(elevation²). Bold represents the optimal model based on AIC. *: $P < 0.01$.
19

20 **Table S6** AIC value for predicting the relationship between phyllosphere microbial Shannon
21 index and elevation (elevation²). Bold represents the optimal model based on AIC. *: $P < 0.01$.
22

23 **Table S7** The direct, indirect, and total standardized effects of mean annual temperature and leaf
24 functional traits on phyllosphere bacterial and fungal richness derived from the pierce structural
25 equation models. Models are presented in Fig. 4. Only significant effects are shown.
26

27 **Table S8** The direct, indirect, and total standardized effects of mean annual temperature and leaf
28 functional traits on phyllosphere bacterial and fungal Shannon index derived from the pierce
29 structural equation models. Models are presented in Fig. S5. Only significant effects are shown.
30
31
32
33
34
35
36
37
38
39
40
41
42
43
44
45
46
47
48
49
50
51
52
53
54
55
56
57
58
59
60

1
2
3
4
5
6
7
8
9
10
11
12
13
14
15
16
17
18
19
20
21
22
23
24
25
26
27
28
29
30
31
32
33
34
35
36
37
38
39
40
41
42
43
44
45
46
47
48
49
50
51
52
53
54
55
56
57
58
59
60

Fig. S2

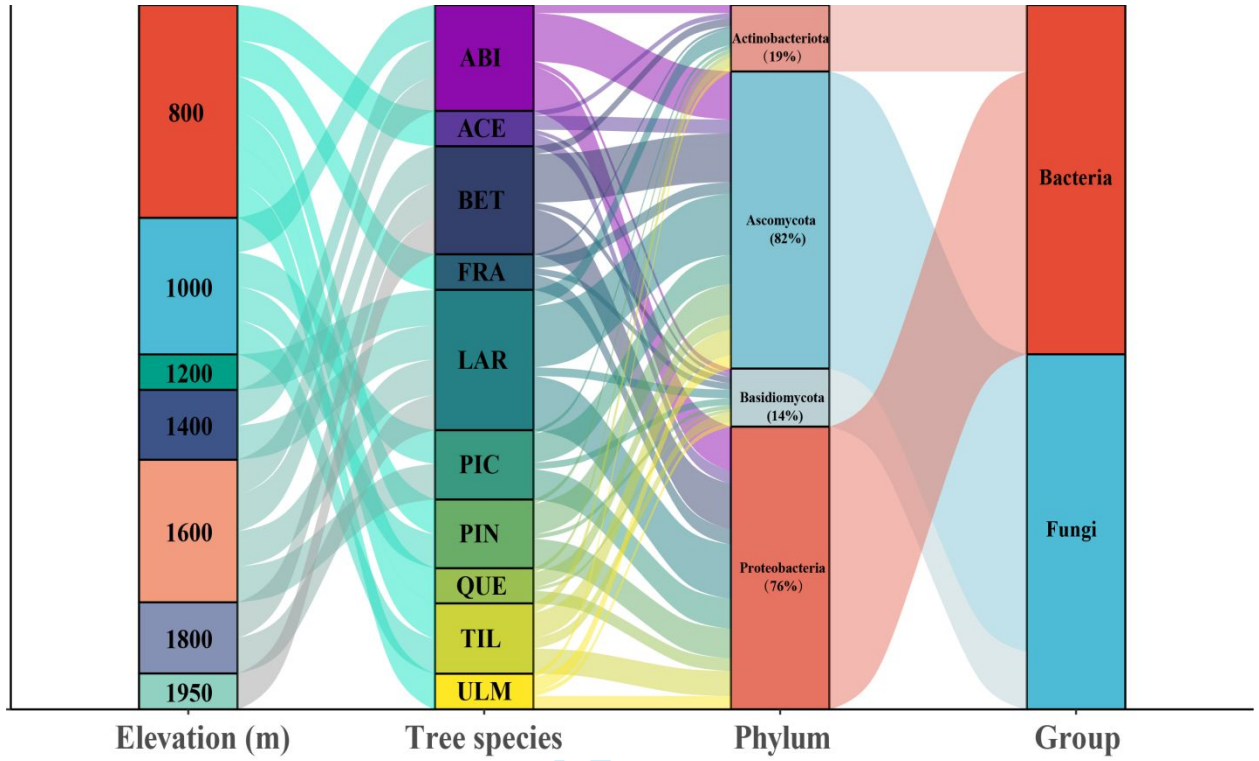
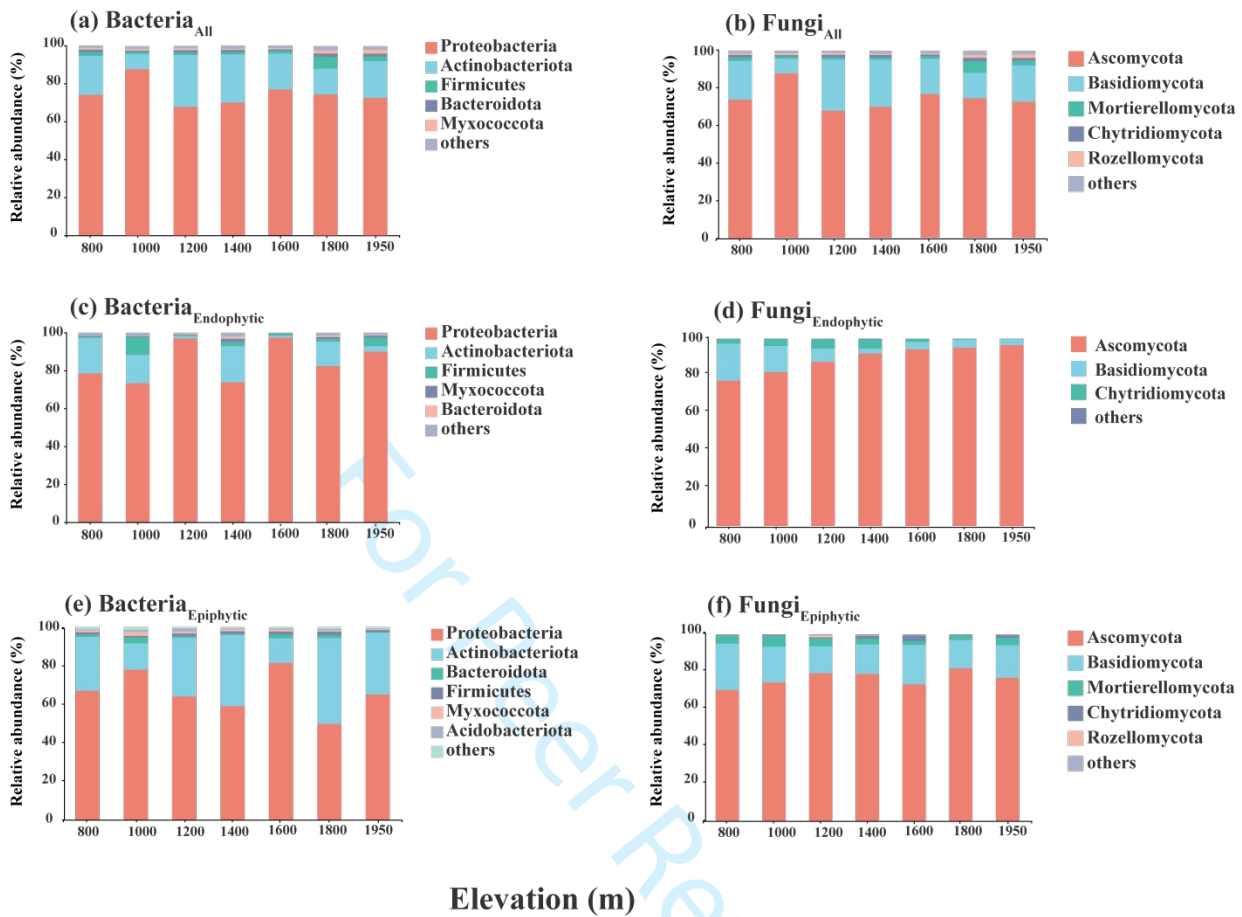
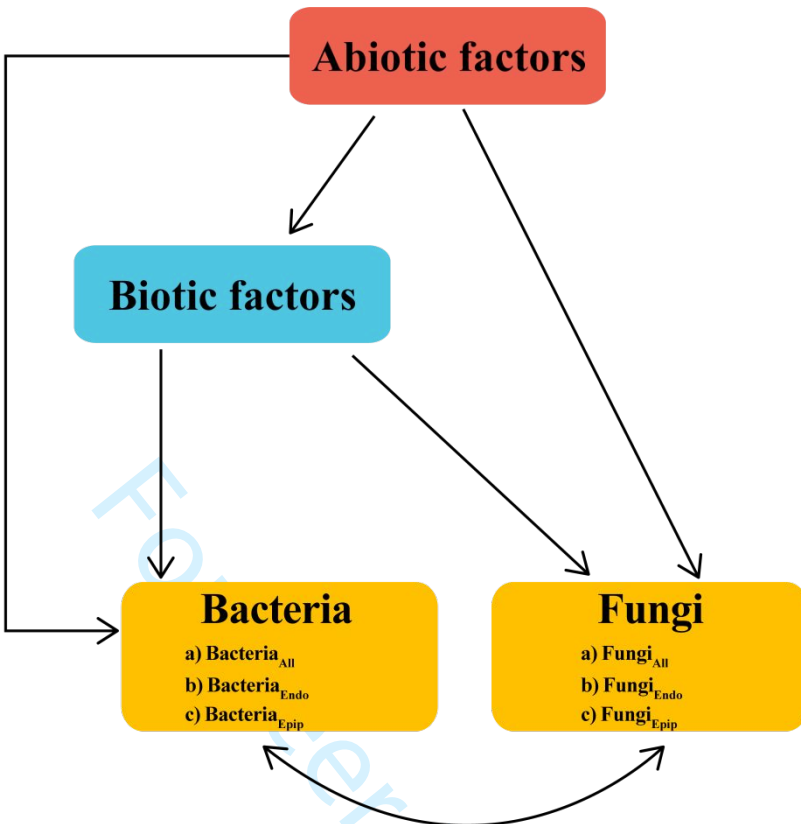


Fig. S3



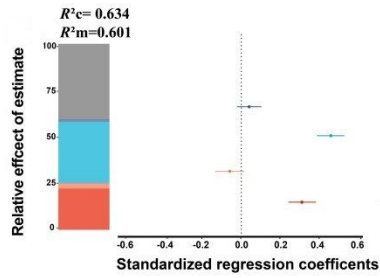
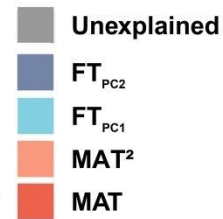
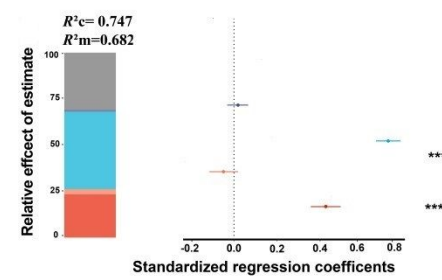
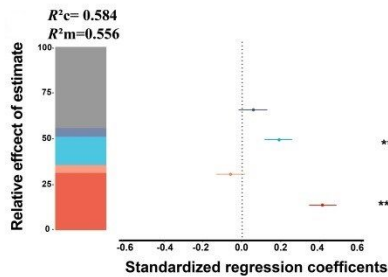
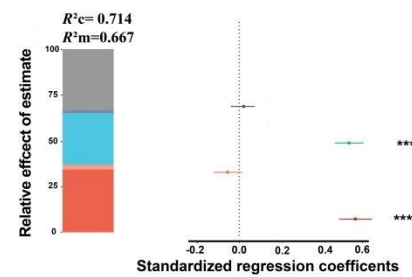
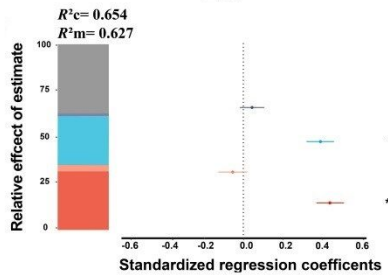
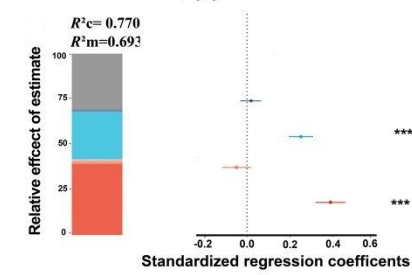
1
2
3
4
5
6
7
8
9
10
11
12
13
14
15
16
17
18
19
20
21
22
23
24
25
26
27
28
29
30
31
32
33
34
35
36
37
38
39
40
41
42
43
44
45
46
47
48
49
50
51
52
53
54
55
56
57
58
59
60

Fig. S4



Pre-Review

Fig. S5

a) H of Bacteria_{All}b) H of Fungi_{All}c) H of Bacteria_{Endo}d) H of Fungi_{Endo}e) H of Bacteria_{Epip}f) H of Fungi_{Epip}

view

Fig. S6

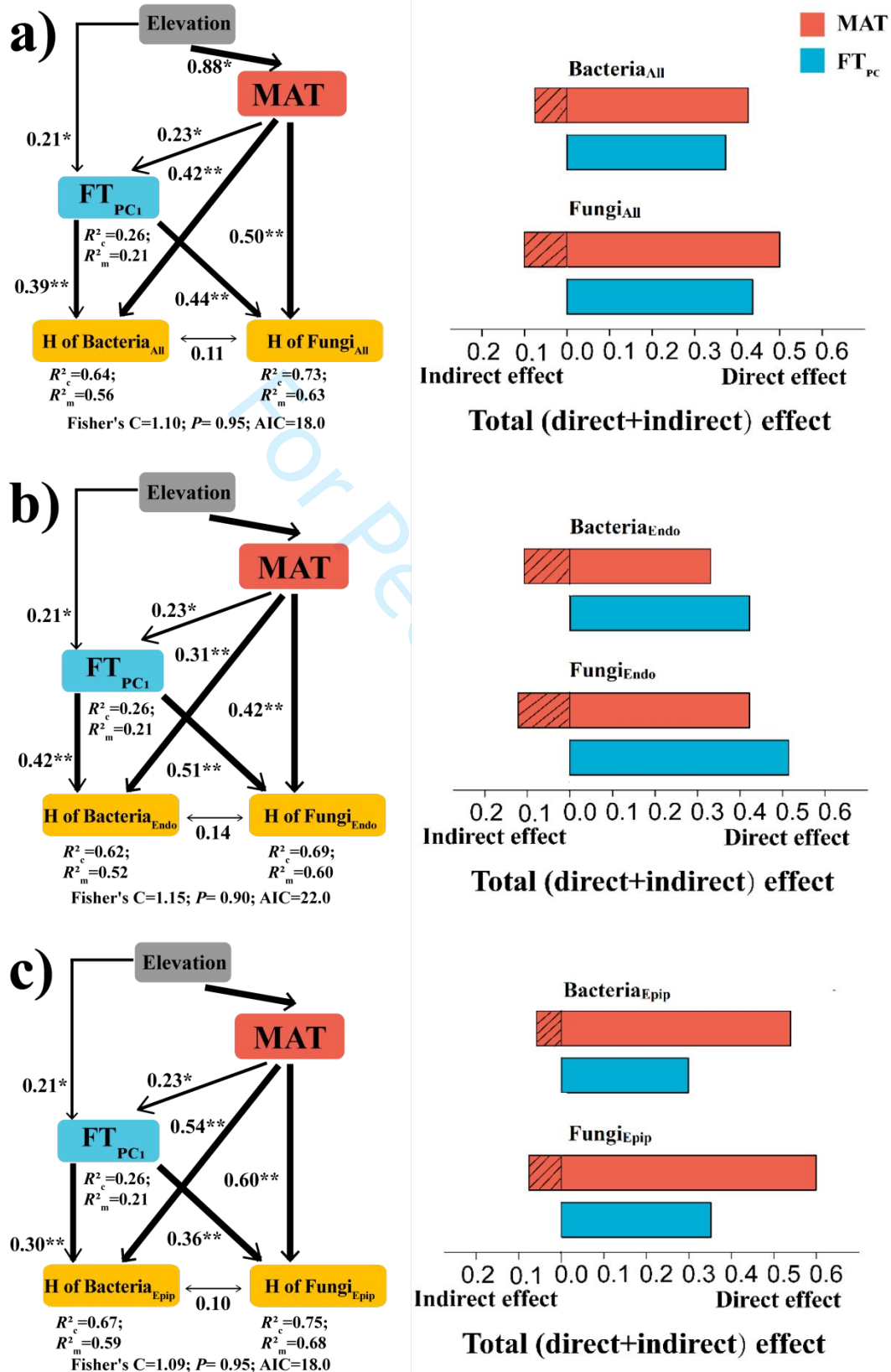


Fig. S7

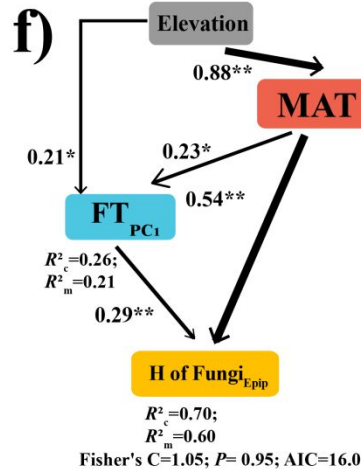
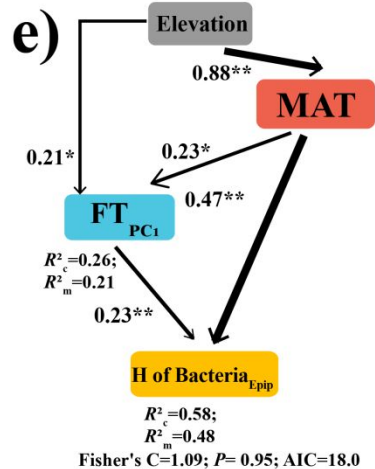
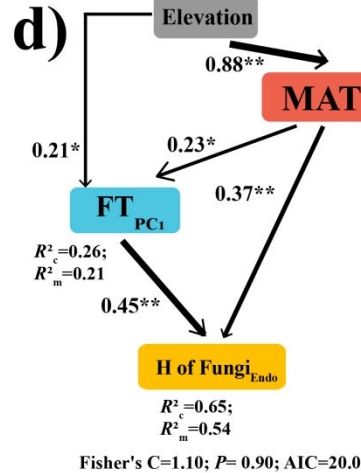
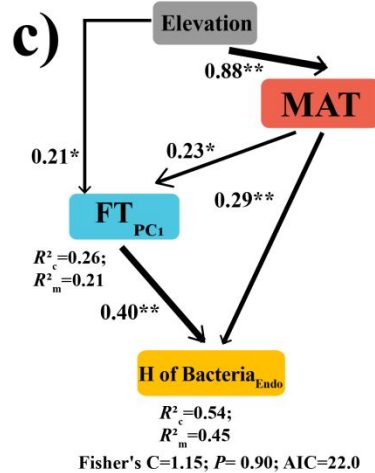
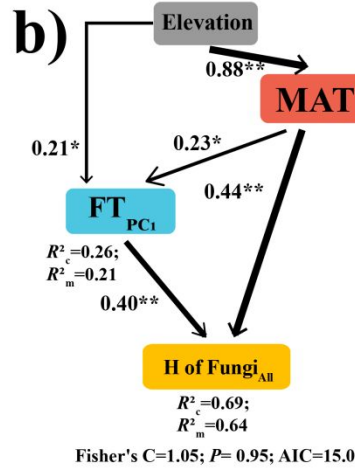
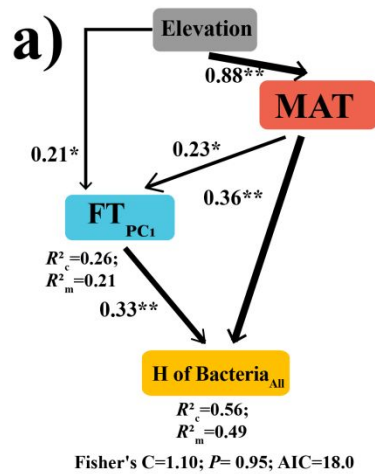


Fig. S8

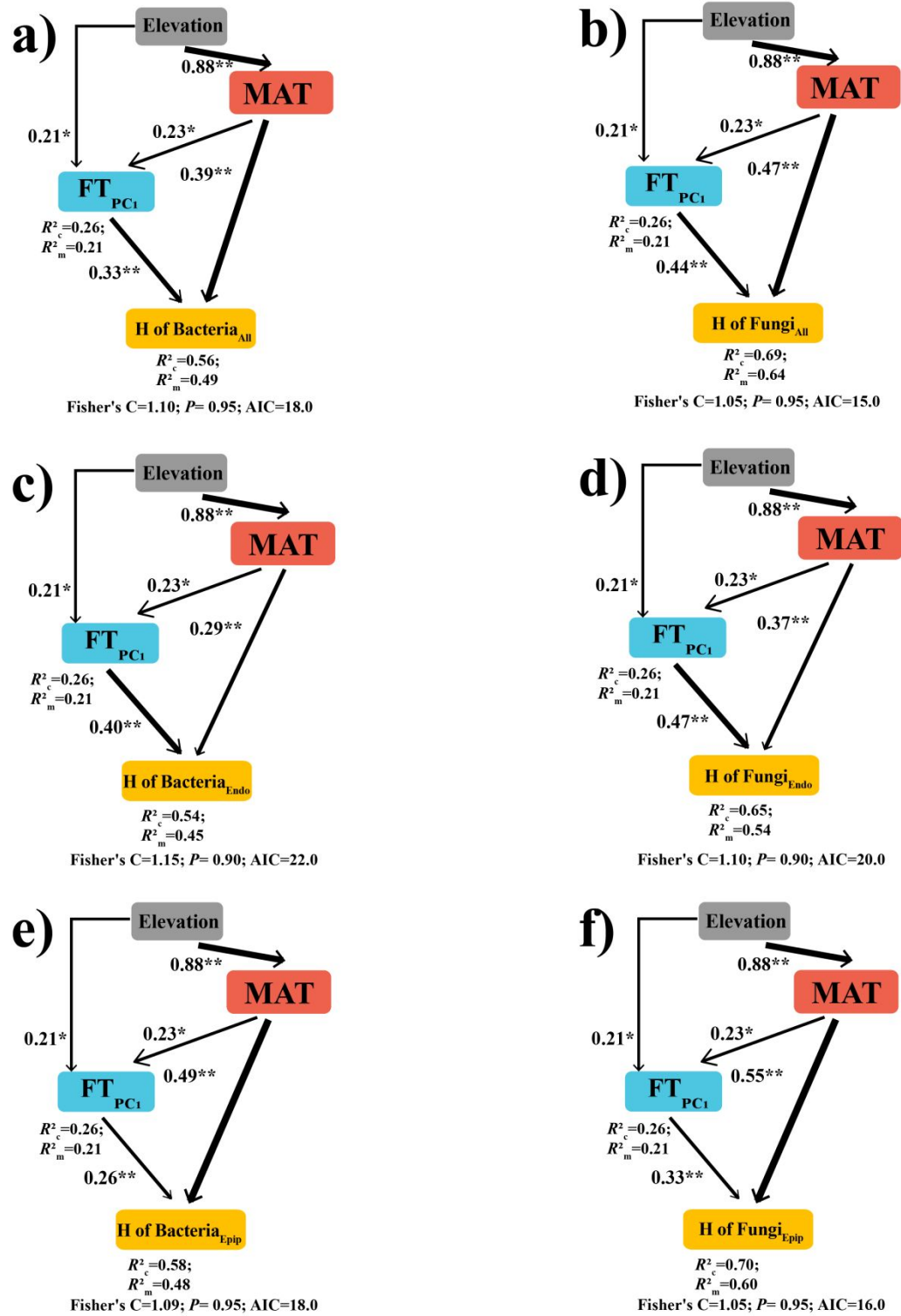
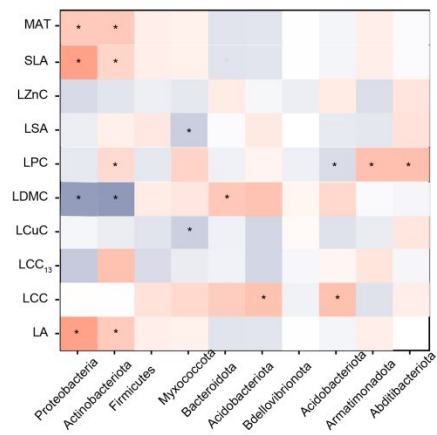
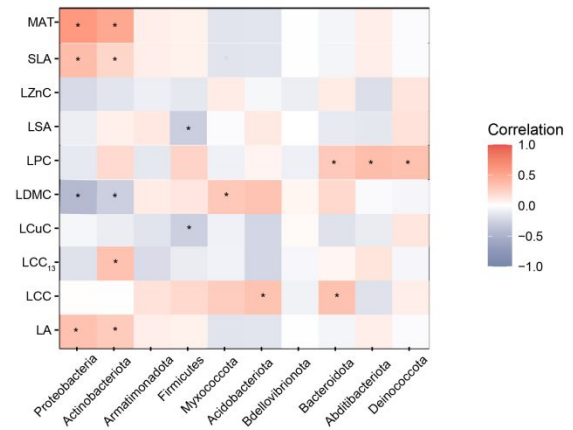


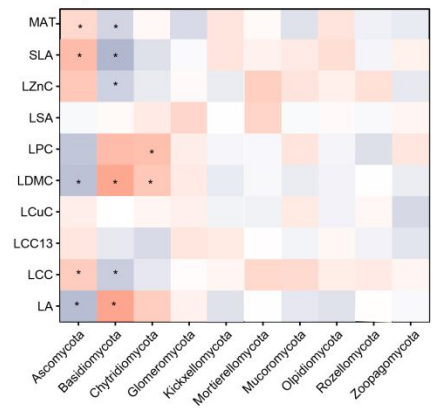
Fig. S9
a)



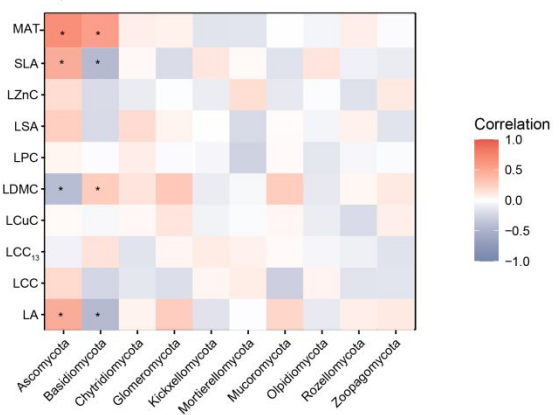
b)



c)



d)



view

Table S1

Elevation	Vegetation type	Tree species name	Abbreviation
800m	<i>Mixed coniferous– broadleaf forest</i>	<i>Ulmus_japonica</i>	<i>ULM</i>
		<i>Quercus_mongolica</i>	<i>QUE</i>
		<i>Acer_mono</i>	<i>ACE</i>
		<i>Tilia_amurensis</i>	<i>TIL</i>
		<i>Pinus_koraiensis</i>	<i>PIN</i>
1000m	<i>Mixed coniferous– broadleaf forest</i>	<i>Fraxinus_mandshurica</i>	<i>FRA</i>
		<i>Pinus_koraiensis</i>	<i>PIN</i>
		<i>Tilia_amurensis</i>	<i>TIL</i>
		<i>Abies_nephrolepis</i>	<i>ABI</i>
1200m	<i>Coniferous forest</i>	<i>Picea_jezoensis</i>	<i>PIC</i>
		<i>Larix_gmelinii</i>	<i>LAR</i>
1400m	<i>Coniferous forest</i>	<i>Abies_nephrolepis</i>	<i>ABI</i>
		<i>Larix_gmelinii</i>	<i>LAR</i>
1600m	<i>Coniferous forest</i>	<i>Betula_ermanii</i>	<i>BET</i>
		<i>Abies_nephrolepis</i>	<i>ABI</i>
		<i>Larix_gmelinii</i>	<i>LAR</i>
		<i>Picea_jezoensis</i>	<i>PIC</i>
1800m	<i>Birch forest</i>	<i>Larix_gmelinii</i>	<i>LAR</i>
		<i>Betula_ermanii</i>	<i>BET</i>
1950m	<i>Birch forest</i>	<i>Betula_ermanii</i>	<i>BET</i>

Table S2

Plot	Latitude	Longitude	Elevation
1	42.2124041	128.4214579	800
2	42.2111062	128.4297998	800
3	42.35094433	127.9687601	800
4	42.3509615	127.9657993	800
5	42.3515333	127.961157	800
6	42.23425683	128.1452635	1000
7	42.23435033	128.1487417	1000
8	42.2399925	128.139942	1000
9	42.235203	128.155823	1000
10	42.23456183	128.151056	1000
11	42.16324833	128.1575617	1200
12	42.1641135	128.1527838	1200
13	42.16171583	128.1496682	1200
14	42.16287717	128.1505947	1200
15	42.16145717	128.1504003	1200
16	42.1111685	128.1021245	1400
17	42.11104967	128.1034917	1400
18	42.11009183	128.1035272	1400
19	42.11084033	128.1009102	1400
20	42.11062467	128.1025682	1400
21	42.0883485	128.0724015	1600
22	42.08745117	128.0736145	1600
23	42.08791617	128.0714043	1600
24	42.08721617	128.0710297	1600
25	42.08674417	128.0724183	1600
26	42.0671645	128.0676052	1800
27	42.06625783	128.0674132	1800
28	42.06493917	128.0665682	1800
29	42.06547567	128.0670377	1800
30	42.06414983	128.067009	1800
31	42.06086367	128.0684068	1950
32	42.06011817	128.0182908	1950
33	42.0597485	128.0676098	1950
34	42.05933067	128.0679163	1950
35	42.058869	128.0683998	1950

Table S3

Abbreviations	Functional traits	Functions
LA	Leaf Area	Resource allocation capacity
SLA	Specific Leaf Area	Resource allocation capacity
LDMC	Leaf Dry Matter Content	Resource allocation capacity
LCC ₁₃	Leaf Stable Carbon 13 Content	Water utilization efficiency
LNC ₁₅	Leaf Stable Nitrogen 15 Content	Resource utilization efficiency
LCC	Leaf Carbon Content	Plant photosynthesis
LNC	Leaf Nitrogen Content	Plant photosynthesis
LPC	Leaf Phosphorus Content	Plant photosynthesis
LKC	Leaf Potassium Content	Plant photosynthesis
LCaC	Leaf Calcium Content	Plant metabolism
LMnC	Leaf Manganese Content	Plant metabolism
LCuC	Leaf Copper Content	Plant metabolism; resistance to diseases, pests and microbes
LZnC	Leaf Zinc Content	Plant metabolism; resistance to diseases, pests and microbes
LSA	Leaf Stomatal Area	Transpiration, photosynthesis

Table S4

Traits	PC1	PC2
	(46.9%)	(28.7%)
LA	0.45	
SLA	0.51	-0.28
LDMC	-0.40	
LCC	-0.40	
LPC	-0.39	-0.33
LCuC		0.592
LZnC		0.649
LCC ₁₃		
LSA		

Table S5

	Predictors	AIC	Likelihood ratio test (Elevation vs. Elevation²)
All bacterial richness	Elevation	234.673	< 0.001
	Elevation ²	274.379	
Endophytic bacterial richness	Elevation	224.673	< 0.001
	Elevation ²	254.142	
Epiphytic bacterial richness	Elevation	227.824	< 0.001
	Elevation ²	265.015	
All fungal richness	Elevation	183.221	< 0.001
	Elevation ²	202.594	
Endophytic fungal richness	Elevation	179.002	< 0.001
	Elevation ²	194.556	
Epiphytic fungal richness	Elevation	184.017	< 0.001
	Elevation ²	199.754	

Table S6

	Predictor	AIC	Likelihood ratio test
	s		(Elevation vs. Elevation²)
All bacterial Shannon index	Elevation	227.606	< 0.001
	Elevation ²	256.386	
Endophytic bacterial Shannon index	Elevation	211.750	< 0.001
	Elevation ²	242.786	
Epiphytic bacterial Shannon index	Elevation	220.554	< 0.001
	Elevation ²	246.012	
All fungal Shannon index	Elevation	179.665	< 0.001
	Elevation ²	203.457	
Endophytic fungal Shannon index	Elevation	169.014	< 0.001
	Elevation ²	187.581	
Epiphytic fungal Shannon index	Elevation	180.171	< 0.001
	Elevation ²	188.600	

Table S7

	MAT	MAT	MAT	FT_{PC1}
	(Total)	(Direct)	(Indirect)	
All bacteria	0.476	0.395	0.081	0.358
Endophytic bacteria	0.399	0.305	0.094	0.417
Epiphytic bacteria	0.582	0.524	0.058	0.258
All fungi	0.567	0.474	0.093	0.412
Endophytic fungi	0.498	0.388	0.110	0.491
Epiphytic fungi	0.647	0.572	0.075	0.333

FOXP Peer Review

Table S8 The direct, indirect, and total standardized effects of mean annual temperature and leaf functional traits on phyllosphere bacterial and fungal Shannon index derived from the piecewise structural equation models. Models are presented in Fig. 5. Only significant effects are showed.

	MAT (Total)	MAT (Direct)	MAT (Indirect)	FT_{PC1}
All bacteria	0.508	0.421	0.087	0.386
Endophytic bacteria	0.403	0.308	0.095	0.423
Epiphytic bacteria	0.603	0.535	0.068	0.304
All fungi	0.629	0.531	0.098	0.436
Endophytic fungi	0.538	0.424	0.114	0.508
Epiphytic fungi	0.684	0.603	0.081	0.359